NASA Contractor Report 182093

PROPULSION SIMULATION FOR MAGNETICALLY-SUSPENDED WIND TUNNEL MODELS

Prakash B. Joshi, Henry P. Beerman, James Chen, Robert H. Krech, Andrew L. Lintz, and David I. Rosen

PHYSICAL SCIENCES INC.
Andover, Massachusetts

Contract NAS1-18616
October 1990

National Aeronautics and Space Administration

Langley Research Center
Hampton, Virginia 23665-5225

PROPULSION SIMULATION
FOR
MAGNETICALLY-SUSPENDED WIND TUNNEL MODELS

Phase I
Final Report

Prepared by:

Prakash B. Joshi
Henry P. Beerman
James Chen
Robert H. Krech
Andrew L. Lintz
David I. Rosen

Physical Sciences Inc.
Research Park, P.O. Box 3100
Andover, MA 01810

Submitted to:

National Aeronautics and Space Administration
Langley Research Center
Hampton, Virginia 23665-5225

PROJECT SUMMARY

In the Phase I program, PSI investigated the feasibility of simulating propulsion-induced aerodynamic effects on scaled aircraft models in wind tunnels employing Magnetic Suspension and Balance Systems (MSBS). The investigation concerned itself with techniques of generating exhaust jets of appropriate characteristics. The influence of aircraft intakes was not addressed in the preliminary study. The specific objectives of Phase I were to:

1. Define thrust and mass flow requirements of jets

2. Evaluate techniques for generating propulsive gas within volume limitations imposed by magnetically-suspended models

3. Conduct simple diagnostic experiments for techniques involving new concepts

4. Recommend experiments for demonstration of propulsion simulation techniques in Phase II.

Toward accomplishing the above objectives, general requirements on thrust and mass flow rates were first established for typical aircraft engine operating conditions. Various gas generation techniques were then examined to simulate the aircraft propulsive jets. Four basic concepts of propulsion simulators were developed: compressed gas cylinders, liquid propellant gas generators, solid propellant gas generators, and some laser-assisted propulsive thrusters. All concepts were based on considerations of compatibility with wind tunnel models (e.g., compactness), compatibility with MSBS characteristics (e.g., remote-activation, lightweight, controllable thrust versus time), and compatibility with wind tunnel facilities (e.g., non-toxic, non-corrosive exhaust). For each propulsion simulator, a conceptual design was developed which identified principal components, mechanism of operation, envelope dimensions and weight estimates.

Very briefly, the basic ideas behind the four propulsion simulation concepts are as follows. The compressed gas concept uses a pressurized cylinder of liquefied carbon dioxide, which is punctured and the resulting CO_2 vapor at regulated pressure is expanded through a nozzle. This concept is simple, but its limitation is that the jet is cold and temperature effects cannot be simulated. The liquid propellant concept utilizes catalytic decomposition of high purity hydrogen peroxide to produce steam and oxygen at high temperatures (~ 1000°K). Although mechanically more complex, this technique is versatile in producing jets having a range of temperatures and pressure ratios. The solid propellant concept uses a formulation which generates an essentially particle-free jet of very high temperature (~ 2500°K). The main limitation is that the jet cannot be turned off and restarted. Out of a number of laser-assisted propulsion simulation concepts, jet generation by ablating material is the most attractive from the viewpoint of mechanical simplicity. Some promising ablator materials were tested to measure their thrust generation and mass flow characteristics under laser irradiation. In all cases, the laser power required was found to be very high (tens of kilowatts) even for the most

modest thrust and mass flows. The report discusses the laser-assisted propulsion simulation technique in more detail. Finally, a comparative evaluation of various propulsion simulators was made relative to a number of criteria of relevance to a Phase II demonstration.

On-board propulsion simulation on magnetically suspended models provides an ideal experiment for accurate measurement of jet-induced forces and moments, free from support interference, on a variety of vehicle and propulsion system configurations. Thus, the proposed research promises to greatly increase the capability and utility of existing and future magnetic suspension wind tunnels. Furthermore, the high quality database developed in these tunnels on propulsion-induced effects will be available for use by the aircraft design community.

TABLE OF CONTENTS

LIST OF FIGURES

LIST OF FIGURES (Continued)

LIST OF TABLES

1. INTRODUCTION

The wind tunnel has been an indispensable tool for aeronautical research and aircraft configuration development for the past 80 years. During that period, tunnels have evolved in speed, increased in size, improved in flow quality, advanced in flow measurement techniques, and became sophisticated in the use of digital computers for data acquisition, reduction, and analysis. Throughout this advancement, the ability of the wind tunnel to faithfully simulate the aerodynamic forces and moments on a model, which can be related to the forces and moments on the full-scale aircraft, has always been limited by uncertainties in measurements due to support and wall interference effects. Support interferences can lead to significant errors in measured aerodynamic force and moment coefficients and static stability derivatives. These errors become very large at transonic speeds and high angles of attack.[1]

Magnetic Suspension and Balance System (MSBS) technology was originally developed in the early 1960's to eliminate the support interference problems. Other potential advantages of MSBS's such as the measurement of dynamic stability derivatives, two-body forces (i.e., aerodynamic interference), simulation of three-dimensional wake flows, were recognized during the subsequent years. However, about 25 years ago, wind tunnel development shifted emphasis from MSBS's to cryogenic tunnels which can duplicate the full-scale flight Mach and Reynolds numbers simultaneously. This capability has recently become available with the completion of the National Transonic Facility at NASA LaRC. Now, the community of experimentalists is advocating the development of MSBS's for large wind tunnels including the cryogenic tunnels. Further impetus for this development has been provided by advancements in the technologies of superconductivity, control systems, and computers.

One of the capabilities desired in wind tunnels employing MSBS's is the simulation of propulsion-induced aerodynamic forces and moments, which arise as a result of interactions between propulsive jets and the free stream. Such a simulation has always been difficult, even in conventional wind tunnels. The main reasons are the problems of introducing high pressure air into the

model and the necessity to make part of the model (where the air lines connect) non-metric. The evaluation of contribution of the non-metric portion to total force/moment measurements, without extensive pressure instrumentation, is difficult at best. In particular, the drag measurement is in serious error because the aircraft's afterbody contributes significantly to its total drag.

The simulation of propulsion on magnetically-suspended models presents special practical problems since there can be no physical connection between a compressed air reservoir and the model. Thus, propulsive gases must be generated onboard the model and then exhausted as the main engine jet or as other jets (such as VTOL lift or thrust reverser jets), Figure 1. The problem involves first defining proper thrust (mass flow rate and velocity) requirements for propulsion jet, and second, using gas generation techniques appropriate for the model size and MSBS wind tunnel facility under consideration.

This report addresses techniques of propulsion simulation which can be employed on models in magnetic suspension wind tunnels. The emphasis here is almost entirely generating exhaust jets with desired characteristics. The issue of simulating engine intake flow (or its matching with nozzle exit flow, for that matter) is touched upon only very briefly and only in a conceptual sense.

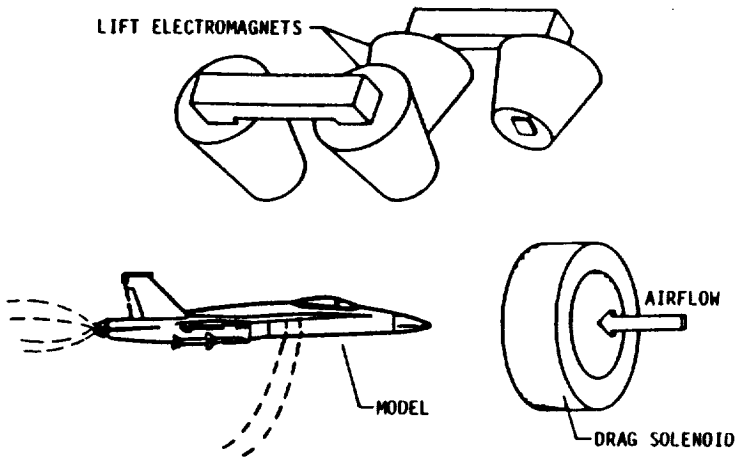

Figure 1. Schematic of Propulsion Simulation on a Magnetically-Suspended Model

2. MOTIVATION AND BACKGROUND

The principal motivation behind the desire to simulate the propulsion system on a wind tunnel model is to study the effect of engine inlet and exhaust flowfields on the aerodynamics of the aircraft. An aircraft designer is interested in the forces and moments induced on the airframe by propulsive components and also in the resulting changes in its stability and control characteristics over the flight envelope. In this context, the generation of exhaust jets on a MSBS wind tunnel model is aimed at simulating the induced aerodynamic forces and not at the simulation of model motion due to application of thrust.

Figure 2 shows schematically a typical aircraft configuration with propulsive jets for different flight regimes. The jets induce forces on the aircraft as a result of the pressure distribution established by their interaction with the free stream in the presence of solid surfaces. The latter can be the wing, fuselage, empennage, or the ground plane. On a fundamental fluid mechanics level, the interaction can be described in terms of turbulent free

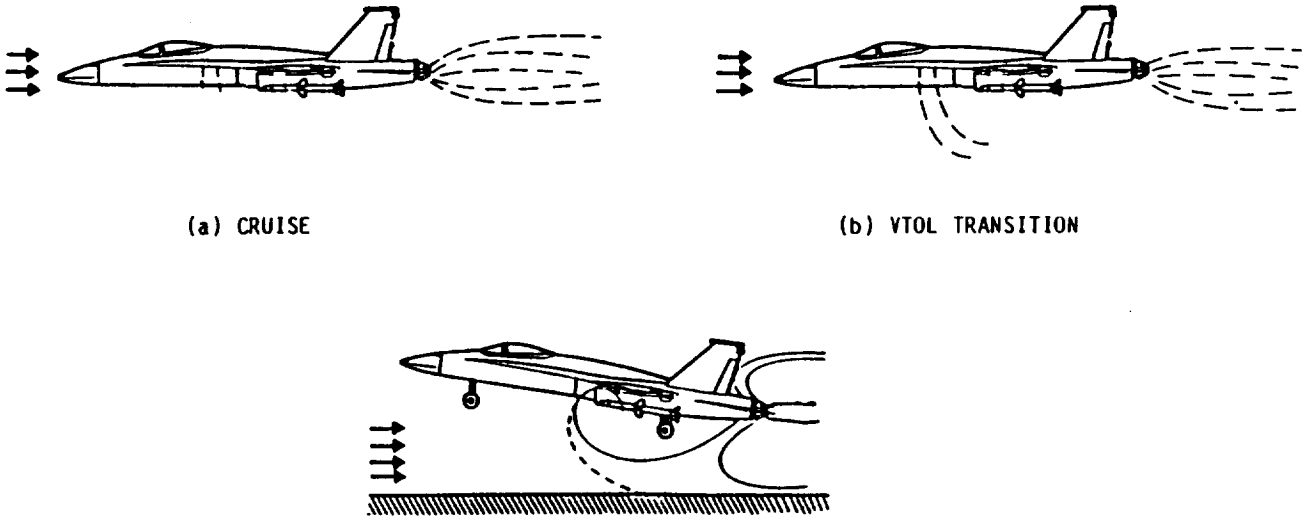

Figure 2. Examples of Propulsive Jet Configurations

shear flows, mixing of streams, jet impingement on a plane surface and wall jet formation, etc. From an engineering point of view, such a description is not only complex but often unnecessary, and consequently, the jet-free stream interaction can be modeled qualitatively in terms of three basic mechanisms. These mechanisms are described briefly below to give the reader a physical insight into the nature of jet-induced flowfields which need to be simulated on an aircraft configuration. Reference 2 may be consulted for details.

Entrainment

This is a process by which free stream fluid is drawn or entrained into a jet of substantially greater velocity. Entrainment occurs at a result of the shear forces at the interface of the two streams and the rate of change of jet momentum along its path. On an aircraft, the entrained fluid comes from neighboring surfaces, primarily aft fuselage, horizontal and vertical tails, and the trailing edge flaps on the wing. The jet-induced flow establishes a pressure distribution and as a result, incremental forces on the aircraft. This would be the case in the cruise mode shown in Figure 2a and the major effect is on aircraft afterbody drag.

Blockage

This process represents the extent to which a jet appears as a solid obstacle to the free stream. The free stream decelerates ahead of the obstacle and accelerates around it. This is the situation, for example, in the VTOL transition regime, Figure 2b. Depending on the location and orientation of the jet relative to various solid surfaces, a pressure distribution and force increment is established by the blockage-induced flow. Whereas entrainment is a strong function of the relative velocities between two streams, blockage primarily depends on the mass flow rate and jet orientation. Figure 3 shows schematically the blockage and entrainment regions for a circular jet in crossflow.

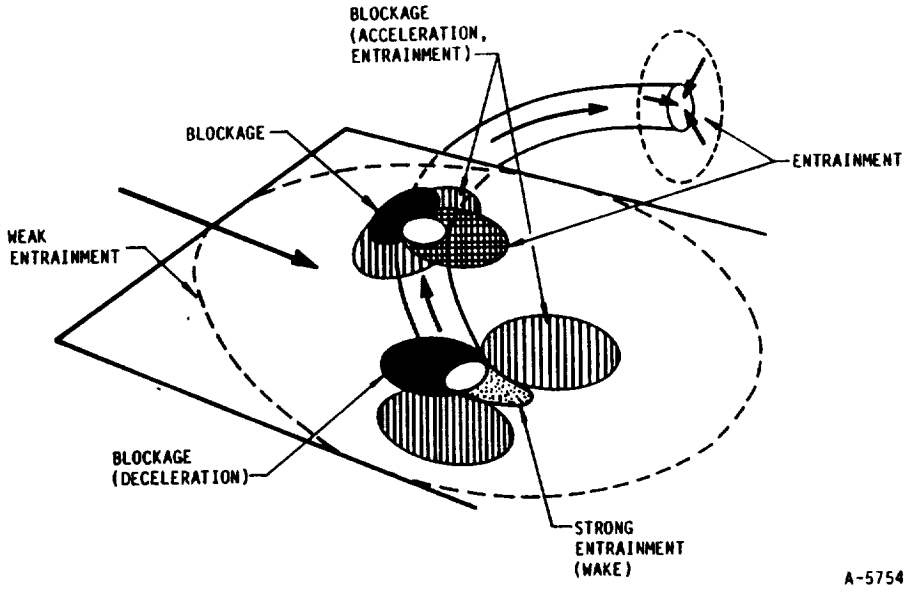

Figure 3. Blockage and Entrainment Dominated Regions for a Circular Jet in Cross Flow

Impingement/Attachment

As the term implies, impingement induces forces on a surface by direct transfer of momentum. This may occur, for example, if the upper thrust reverser jets in Figure 2c move laterally due to a cross wind and impinge or attach to the vertical tails. Jet attachment rather than impingement can also occur when a jet issues at shallow angles relative to a surface. Jet impingement can sometimes occur in the presence of a ground plane as shown in Figure 2c during approach and landing or VTOL operations close to ground. The flowfield resulting from the impingement induces forces and moments on the aircraft which are unsteady and potentially very large.[3]

In practice, the jet-free stream interaction mechanisms described above operate simultaneously. They form the physical basis for propulsion-induced aerodynamic forces on an aircraft. The problem of propulsion simulation, therefore, does not entail as much the generation of a thrust force as it does the simulation of the flowfield which is associated with that force. This flowfield can be ascribed certain characteristic non-dimensional parameters which are discussed in the next section.

3. STATEMENT OF THE PROBLEM AND PHASE I OBJECTIVES

As mentioned earlier, proper simulation of inlet/exhaust flows is an inherently difficult technical problem. There are also questions regarding appropriate scaling parameters for jet/free stream and jet/airframe flowfield interactions. Magnetically-suspended models impose further challenges as described in the following paragraphs.

First and foremost, existing MSBS wind tunnels allow the installation of relatively small models, which results in a limited volume available for a propulsion simulation device. Since the magnetic core used for levitation also needs some space within the model, the restrictions on the size of the propulsion (i.e., engine) simulator can indeed be significant. For example, the largest operational MSBS wind tunnel in the U.S. at NASA Langley Research Center has a 13-in. diameter test section. Another MSBS facility at University of Southampton, England, which is more versatile in that it has angle-of-attack variation capability, has only a 7 in. wide test section. In this wind tunnel, the model envelope would typically be 5 to 6 in. length with 1 to 1.5 in. diameter centerbody. In the NASA tunnel, models 15 in. long by 2 in. diameter can be installed.

The volume limitation directly translates into the mass of the propellant for exhaust jet generation which is carried onboard the model. In turn, this limits the duration over which the exhaust jet can be maintained. For practical applications, this means frequent model refurbishing and thus potentially reduced tunnel productivity with propulsion simulation.

Since no physical connections exist with a magnetically-levitated model, it is necessary to control the propulsive module remotely. Therefore, the source of electrical energy required to open/close valves or initiate ignition must either be carried onboard and triggered externally by such means as radio control or lasers.

The characteristics of a particular MSBS also impose some restrictions on the propulsion simulator. These are the weight of the simulator module which can be suspended and the level of thrust force. The restrictions arise due to the limitations on the amount of current which can be driven through the coils of the external electromagnets (Figure 1). Another consideration is that the thrust rise (or fall) time, when propulsion is turned on (or off), must be controllable by the control system of the MSBS.

Finally, any propulsive gas generation technique must be compatible with the particular wind tunnel hardware involved and its operational requirements. As will be discussed in the next section, even small quantities of particulate matter or water vapor in the exhaust may not be acceptable in some facilities. Furthermore, there may be considerations of safety of personnel, requiring special precautions in some cases.

The above considerations led to the following objectives for the Phase I investigation.

The overall goal of the Phase I research was to establish the feasibility of simulating propulsion-induced aerodynamic effects on magnetically-suspended wind tunnel models. Specific Phase I objectives were to:

a. Define thrust and mass flow requirements of propulsive jets

b. Evaluate techniques for generating propulsive gas within volume limitations imposed by magnetically-suspended models

c. Conduct simple diagnostic experiments for techniques involving new concepts.

d. Recommend experiments for demonstration of propulsion simulation techniques in Phase II

4. RESULTS FROM PHASE I INVESTIGATION

4.1 Definition of Thrust and Mass Flow Requirements

4.1.1 Non-Dimensional Scaling Parameters

The simulation of jet-induced effects involves producing a gas jet(s) at a specific geometrically-scaled location(s), with the desired spatial orientation and with appropriate physical characteristics. The spatial orientation of the jet relative to the neighboring aerodynamic surfaces (and the ground plane for an impinging jet) is important because it determines the relative strengths of the jet/free stream interaction mechanisms described in Section 2. The physical characteristics of the jet are primarily its velocity relative to the free stream, its exit cross sectional area relative to that of neighboring surfaces, and its temperature (or density). These parameters fix the mass flow rate and thrust. Jet characteristics of secondary importance include velocity profile across the jet and turbulence level.

The primary physical characteristics of a jet can be expressed in terms of non-dimensional parameters appropriate to a given problem. For example, when simulating the main exhaust jet on an aircraft in cruise mode, Figure 2, this parameter is Jet Pressure Ratio (JPR)

$$JPR = P_{oj}/p_{\infty} \qquad (1)$$

where P_{oj} = stagnation pressure of the jet prior to expansion and p_{∞} = ambient static pressure. The significance of JPR is that it accounts for jet characteristics, such as cross section and velocity profile as the jet mixes with the surrounding fluid and develops downstream. The jet velocity after expansion, relative to the local free stream, determines the entrainment of fluid from the aircraft's afterbody and control surfaces. The jet velocity, V_j, is related to the pressure ratio, for an isentropic expansion to ambient p_{∞}, by

$$V_j = \left[\frac{2\gamma RT_o}{\gamma-1}\right]^{1/2} \sqrt{1 - (P_{oj}/p_\infty)^{(1-\gamma)/\gamma}} \tag{2}$$

where T_o is the stagnation temperature of the jet, γ = specific heat ratio, and R = gas constant of the jet fluid. The thrust is given by

$$T = \dot{m}\, V_j \tag{3}$$

with the mass flow rate $\dot{m}$ expressed in terms of (P_{oj}/p_∞) as

$$\dot{m} = p_\infty\, A^* \frac{(P_{oj}/p_\infty)}{\sqrt{RT_o}} \sqrt{\gamma} \left(\frac{2}{\gamma+1}\right)^{(\gamma+1)/2(\gamma-1)} \tag{4}$$

where A^* is the throat area of the nozzle through which the jet is issuing.

When the simulation of interest is a thrust reverser type jet in a cross flow, as in Figure 2c, where the jet's trajectory must be faithfully represented, the applicable non-dimensional parameter is the dynamic pressure ratio

$$\frac{q_j}{q_\infty} = \frac{\frac{1}{2}\rho_j V_j^2}{\frac{1}{2}\rho_\infty V_\infty^2} \tag{5}$$

where ρ_∞ is the density of free-stream cross flow. The dynamic pressure ratio can be expressed in terms of the jet pressure ratio as

$$\frac{q_j}{q_\infty} = \frac{2}{(\gamma-1)M_\infty^2} \left[\left(\frac{P_{oj}}{p_\infty}\right)^{\frac{\gamma-1}{\gamma}} - 1\right] \tag{6a}$$

or, for a given q_j/q_∞, the corresponding jet pressure ratio is

$$\frac{P_{oj}}{p_\infty} = \left(1 + \frac{\gamma-1}{2} M_\infty^2 q_j\right)^{\frac{r}{r-1}} \quad . \tag{6b}$$

In Eqs. (6a) and (6b), M_∞ is the Mach number of the free stream cross flow. The thrust and mass flow rate follow from Eqs. (3) and (4), respectively.

A non-dimensional parameter sometimes used for V/STOL jets, such as in Figure 2b, is called the momentum ratio

$$C_\mu = \frac{\dot{m} V_j}{q_\infty S_W} \tag{7}$$

where S_W is the area of the surface (e.g., wing) through which the jet is exhausting. The mass flow rate $m = \rho_j A_j V_j$, where A_j = exit area of the jet. C_μ is a particularly useful correlation parameter when the jet area is a significant fraction of the surface area and thus exerts considerable influence on the flow over the surface. Since C_μ can be written as

$$C_\mu = \left(\frac{q_j}{q_\infty}\right)\left(\frac{A_j}{S_W}\right) \tag{8}$$

its relationship to the dynamic pressure ratio and the jet pressure ratio can be established from Eqs. (8) and (6a), if necessary.

In the above discussion, the effect of jet temperature T_{oj} enters through its direct influence on the jet velocity in Eq. (2) or through density in Eq. (5). The effect of jet temperature on the interaction mechanisms and induced forces (Section 2) is not so clear. Ignoring buoyancy effects, which

can be important for hot gas ingestion in VTOL aircraft, temperature is thought to be a parameter of lesser importance than the parameters in Eqs. (1), (5), and (8). Intuitively, it appears that a hot jet will have higher level of turbulence and thus more mixing and greater effect on jet development than a cold jet. For this reason a parameter like T_{o_j}/T_{o_∞}, where T_{o_∞} = free stream stagnation temperature, may be appropriate. The jet simulation techniques discussed in Subsection 4.2 include generation of hot jets.

4.1.2 Thrust and Mass Flow Rate Requirements

Starting with the simplest non-dimensional parameter identified in Subsection 4.1.1, namely the pressure ratio P_{o_j}/p_∞, the following expressions for mass flow rate per unit area (i.e., flux) and thrust per unit area can be derived

$$\frac{\dot{m}\sqrt{RT_o}}{A} = p_\infty \left(\frac{P_{oj}}{p_\infty}\right) \sqrt{\gamma}\left(\frac{2}{\gamma+1}\right)^{(\gamma+1)/2(\gamma-1)} \tag{9}$$

$$\begin{aligned}\frac{T}{A} &= \frac{\dot{m}}{A} V_j \\ &= \left[\frac{2}{\gamma-1}\right]^{\frac{1}{2}} r \left[\frac{2}{\gamma+1}\right]^{(\gamma+1)/2(\gamma-1)} p_\infty \left(\frac{P_{oj}}{p_\infty}\right) \sqrt{1 - \left(\frac{P_{oj}}{p_\infty}\right)^{\frac{1-\gamma}{\gamma}}}\end{aligned} \tag{10}$$

where Eq. (2) has been used. Note that the mass flux depends on temperature but the thrust per unit area does not. The latter is a function of the specific heat ratio and the pressure ratio only. The gas constant R in Eq. (9) is defined by

$$R = \frac{R_{univ}}{M} \tag{11}$$

where R_{univ} = universal gas constant = 1545.3 ft-lbf/lbmole-°R or 8.31×10^7 erg/gm mole-°K, and M = molecular weight of gas.

Equation (9) shows that for a given pressure ratio to be simulated, a high temperature jet would require less mass flux, thus requiring less mass to be carried on board for a given "run time". The opposite is true for a cold jet. The mass requirement can be reduced by using a gas with lower molecular weight, i.e., large gas constant, Eq. (11). This is desirable particularly in view of the typically small volume available for current MSBS wind tunnel models. The role of specific heat ratio (γ) can be determined by plotting Eqs. (9) and (10) for a range of pressure ratios with γ as a parameter. This is shown in Figures 4 and 5. It is seen that the mass flux is weakly dependent upon γ, whereas the thrust per unit area displays little sensitivity to γ.

The pressure ratio range shown in Figures 4 and 5 covers the values for current jet engines, namely 3-4. So typical ranges for mass flow and thrust are:

$$\frac{\dot{m}}{A}\sqrt{RT_o} \simeq 1000 - 1200 \ \frac{lbm}{in.^2\text{-}s} \cdot \frac{ft}{s} \tag{12a}$$

$$\frac{T}{A} \simeq 40 - 50 \ \frac{lbf}{in.^2} \tag{12b}$$

for

$$\frac{P_{oj}}{P_\infty} \simeq 3\text{-}4 \quad . \tag{12c}$$

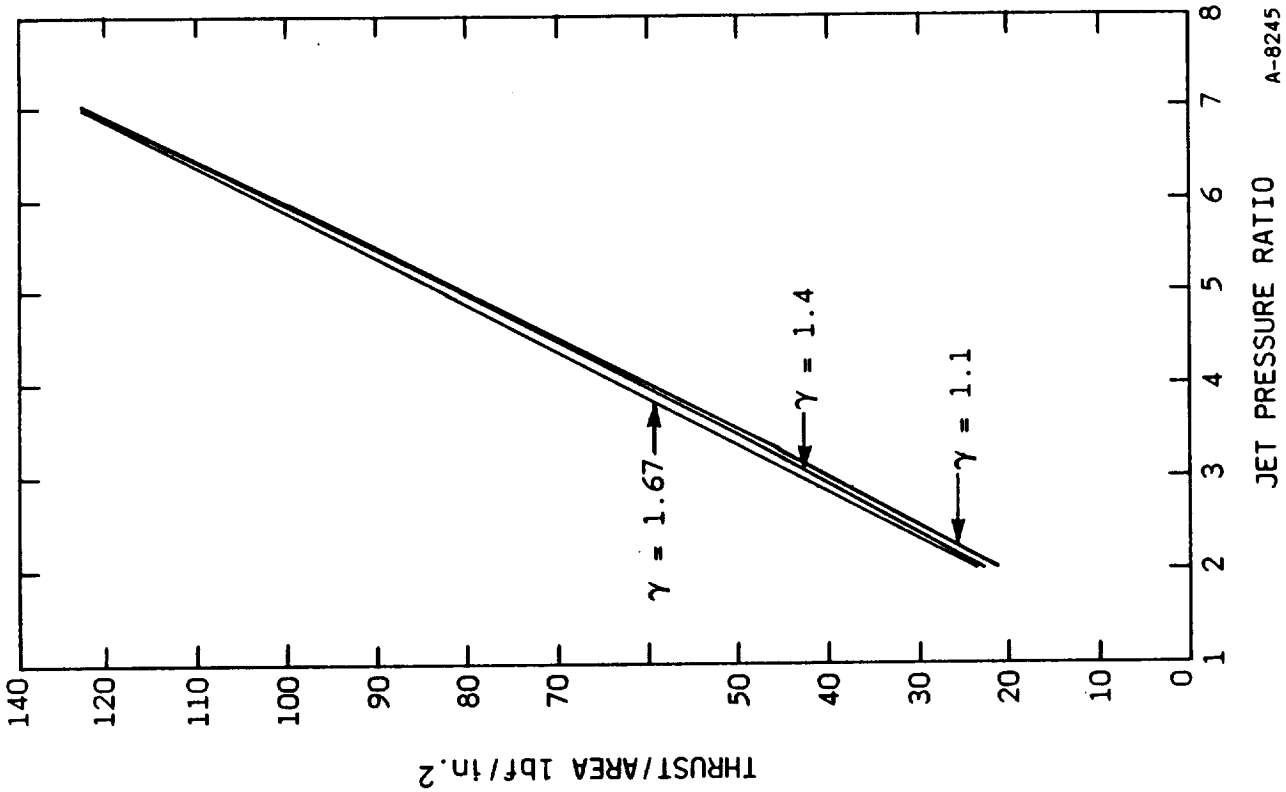

Figure 5. Thrust Per Unit Area Versus Jet Pressure Ratio

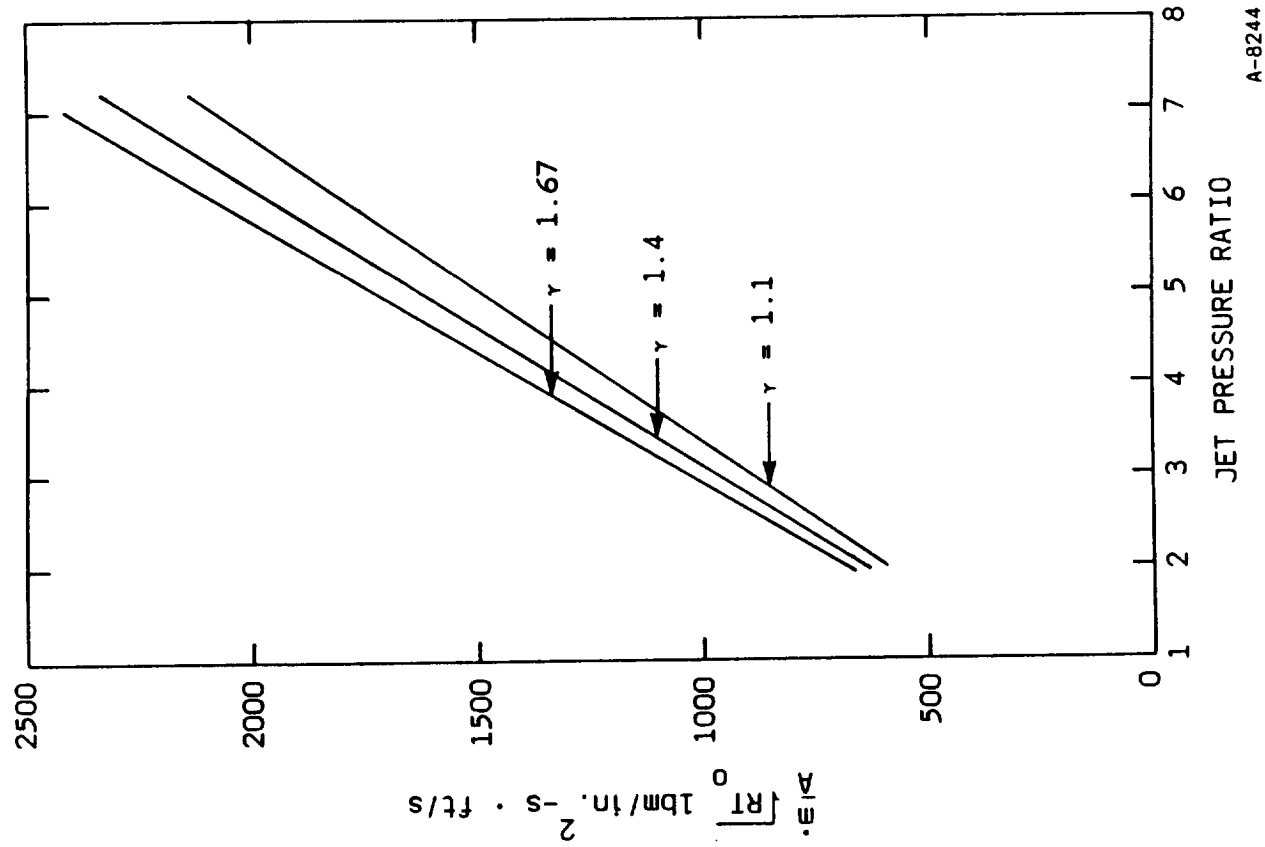

Figure 4. Mass Flux Versus Jet Pressure Ratio

The range of interest for the other important non-dimensional parameter, namely the dynamic pressure ratio in Eq. (6a), is 50-70 as shown in Ref. 2. The jet pressure ratio range of 3-4 roughly covers this dynamic pressure ratio range, as seen from Figure 6 which is constructed from Eq. (6b).

It is of interest to determine the mass flow rates of typical propellant gases from the requirements stated above. For this purpose an exit area for the jet, A, must be chosen. The 1/40-scale throat area for an F-404 engine at maximum power is approximately 0.14 $in.^2$ or 0.43 in. diameter. Table 1 shows the required mass rates for typical gases, carbon dioxide and helium, at room temperature (300°K) and at 1200°K.

It is clear from Table 1 that helium at high temperature has the smallest mass flow rate. However, in a typical 5s run, approximately 60 grams or 15 moles of helium will be needed. For this amount of helium to be carried in a cylinder approximately 1 in. diameter and 5 in. long, the required pressure will be in excess of 5000 atm or density greater than 1 gm/cm^3! As will be

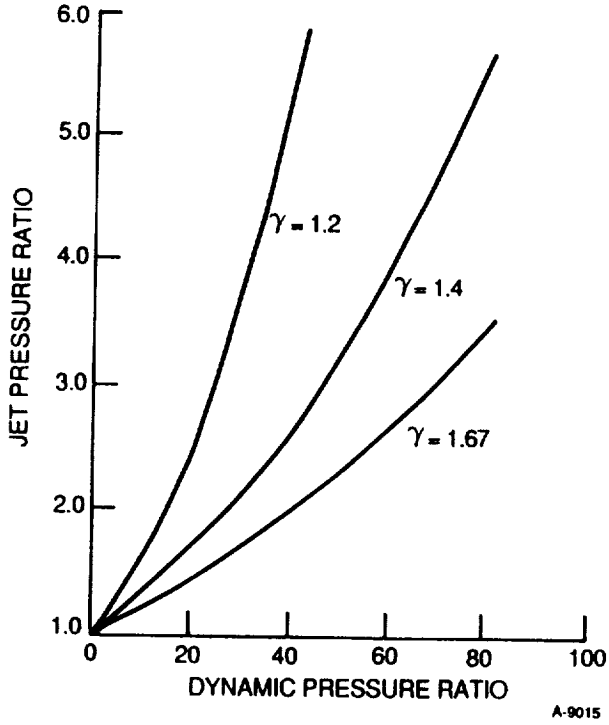

Figure 6. Jet Pressure Ratio Versus Dynamic Pressure for $M_\infty = 0.2$

Table 1. Typical Mass Flow Rate and Thrust Requirements

Gas	Molecular Weight	Mass Flow Rate*, g/s		Thrust (kgf)
		@ T_o = 300°K	@ T_o = 1200°K	
CO_2	44	80-100	40-50	2.5-3.2
He	4	25-30	12-15	2.5-3.2

*A = 0.14 in.^{2} (0.43 in. diameter) with parameters as specified by Eqs. (12a)-(12c)

discussed in Subsection 4.2, carbon dioxide is a more attractive propellant in spite of its greater molecular weight because it can be carried in liquidified form under pressure.

The mass flow requirements in Table 1 must be adjusted if a smaller jet area must be chosen because of model size constraints dictated by common MSBS wind tunnels. A 1/40-scale F-16 (which has the F-404 engine) has a wing span of 9.3 in. which can be accommodated in the 13-in. NASA Langley MSBS tunnel, but not in the University of Southampton tunnel.

4.2 Jet Simulation Techniques

4.2.1 General

In the present context, jet simulation means gas generation and subsequent expansion through a nozzle to provide desired mass flow and thrust. Some general considerations for jet (or propulsion) simulators compatible with MSBS wind tunnels were discussed in Section 2. This section deals with various techniques of jet simulation and discusses the issues pertinent to each technique. The techniques are investigated to establish their feasi-

bility and to develop some conceptual design schemes. General design considerations common to all techniques are summarized in Table 2.

The following four techniques were investigated relative to the considerations listed in Table 2:

1. Compressed gas cylinders
2. Liquid propellant gas generator
3. Solid propellant gas generator
4. Laser-assisted propulsive thrusters.

Each technique will now be described in detail.

Table 2. General Design Considerations for Propulsion Simulators

· Compactness	Smallest size possible for demonstration in currently available MSBS tunnels
· High Density Propellant	Ability to carry the largest propellant mass in a given volume inside the model to maximize run time for a specified mass flow rate
· Relatively Lightweight	To minimize the size of magnetic core within the model and currents in external electromagnets
· Remote or Minimum Interference Activation	If remote activation is not feasible, the disturbance to flow field and magnetic field must be negligibly small
· Thrust Level	Compatible with particular MSBS capability
· Thrust vs. Time Characteristics	Compatible with MSBS control system capability. Stable thrust duration must be sufficiently long so that data can be obtained after model becomes steady.
· Safe Operation	Propellant material should be non-toxic, non-corrosive, with minimum of particulates

4.2.2 Compressed Gas Cylinders

Perhaps the simplest propulsion simulator is a compressed gas cylinder attached to a nozzle and turned on/off by means of a remotely-controlled valve. However, as mentioned in Subsection 4.1.2, the mass of gas which can be carried under reasonable pressures in small volumes typical of a MSBS wind tunnel model is so small that the resulting thrust time (or run time) will be of the order of tens of milliseconds. Furthermore, the gas container will have to be refilled under high pressure innumerable times, which makes this approach impractical.

A way around this problem is to use gases that liquefy easily under pressure at room temperature, so that a significantly larger mass can be stored in a given volume. Among common substances, the candidates are carbon dioxide (CO_2) and Ammonia (NH_3). Table 3 lists the physical properties of these gases along with another substance, sulfur dioxide (SO_2) which has some desirable properties.

The ideal propellant gas should have high density in liquid phase to pack as large mass as possible in a given volume and a low molecular weight (see Eq. (10)). Low heat of vaporization is desired so that, as the liquid changes into vapor, it does not draw such a large amount of heat from itself and

Table 3. Physical Properties of Propellant Gases

Gas	Molecular Weight	Vapor Pressure at 70°F (psi)	Density of Liquid (gm/cm^3)	Heat of Vaporization (cal/gm)
CO_2	44	840	0.75	36
NH_3	17	129	0.61	283
SO_2	64	50	1.38	83

surrounding walls that it will freeze. Low vapor pressure is also desirable, because it means that liquification occurs at lower pressure at a given temperature. Thus, the pressure regulation necessary to drop the pressure to 45 to 60 psia (P_{oj}/p_{∞} = 3-4 in Eq. (12c)) is relatively straightforward. That is, compact regulators, necessary in the present application, are easy to find.

Examination of Table 3 shows that each gas has certain advantages and disadvantages. Ammonia has the lowest molecular weight and reasonably low vapor pressure, but it has extremely high heat of vaporization and the lowest density. Sulfur dioxide, on the other hand, has the lowest vapor pressure and highest density (38% above water), but the latter is offset by its high molecular weight. The heat of vaporization of SO_2 is considerably lower than that of NH_3. Carbon dioxide has a molecular weight between that of NH_3 and SO_2, the lowest heat of vaporization, and density slightly higher than that of ammonia. The biggest disadvantage of CO_2 is its high vapor pressure (56 atm).

There are some practical advantages of CO_2 that make its choice as a propellant almost inevitable. It is commercially available in cartridges (or cylinders) which vary in weight from a few grams to hundreds of grams. The cylinders are very compact, a cylinder containing 16 grams of CO_2 measures 3.5 in. long x 0.865 in. diameter, a 60 gram cylinder measures 5.1 in. long x 1.6 in. diameter. As these cylinders have wide commercial applications (air guns, life vests, inflatable boats, beverage industry), they are available in any desired quantity at a very low cost. For example, the price of a 16 gram CO_2 cylinder is less than $2. Another advantage of these cylinders is that they are available in stainless steel (which is non-magnetic) or as magnetizable steel. This is potentially useful because the mass of the cylinder itself can serve as a part of the magnetic core. CO_2 cylinders can be obtained as customized components from Sparklet Devices, Inc.

CO_2 also has some operational advantages over NH_3 and SO_2. In practice, the mass flow rate of the gases will be small (< 100 gram/s) compared to that in the wind tunnel (~ 2 kg/s in University of Southampton 7 in. tunnel and

7 kg/s in NASA Langley 13 in. tunnel) and the duration will be typically less than 5s for one thrusted run. Thus the propellant gases will get quickly mixed, diluted, and dispersed in the wind tunnel-free stream. In open circuit tunnels, of course, the products will leave the test section and not be circulated. CO_2 is a clean, non-contaminating, non-corrosive and safe gas. NH_3 and SO_2 on the other hand are somewhat corrosive, and can be irritants to eyes and lungs, if released accidentally. The use of these gases then entails special precautions not necessary to CO_2.

Some disadvantages of the compressed gas concept are that miniaturized, remotely operated valves are required to turn the jet on/off, and further, a battery power supply and switch must be incorporated in the limited volume of the model. An inherent limitation of the compressed gas concept is that the total temperature of the jet is close to room temperature. Therefore, a hot jet is not possible unless heat is added before exhausting the gas, which represents an additional complication. The problem of cooling of the cylinder as the liquid vaporizes can be minimized by surrounding the cylinder with an annular magnetic care which can provide the necessary thermal mass.

A conceptual design for a CO_2 jet propulsion simulator is shown in Figure 7. It has an overall envelope of 1 in. diameter x 7 in. length. Principal components are a CO_2 cylinder (16 gram), a cap-piercing fitting which releases the gas from the cylinder to the fast-acting solenoid valve

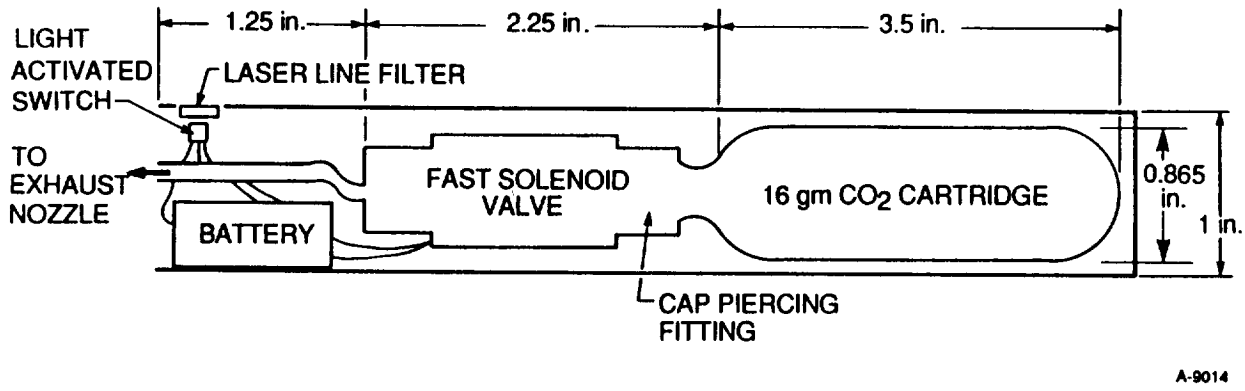

Figure 7. Conceptual Scheme for a CO_2 Jet Simulator

manufactured by General Valve, Inc. This valve has a typical response time of 5 ms, and is opened or closed by a signal from the light activated switch. The switch is activated by a laser, such as a 10 mW, 633 nm HeNe. The pressure and mass flow delivered by the solenoid can be controlled by rapidly opening and closing the solenoid via laser pulses of appropriate width. The solenoid is operated on power supply consisting of a stack of lithium batteries, shown to scale in Figure 7. Tests will have to be performed to determine the laser pulse width, mass flow rate for a given tubing size, tubing length (or additional plenum requirement) to smooth out pulses from the valve, and finally, the run time. The run time can be increased by reducing the jet exit diameter, at least for demonstration purposes in small MSBS wind tunnels. For example, scaling the exit diameter down by a factor of four (i.e., 0.11 in. instead of 0.43 in. in Table 1), will reduce the mass flow rate by a factor of 16, to 5 to 6.25 gm/s, yielding about 3s run time from a 16 gram CO_2 cylinder. Note that for larger scale MSBS tunnels of the future, model volume increases as the cube of its scale, whereas jet exit area increases as the square, and the on-board propellant mass limitations will be much less stringent.

4.2.3 Liquid Propellant Gas Generator

The compressed gas concept just discussed has the inherent limitation that only a "cold" jet (stagnation temperature equal to room temperature) can be generated, unless heat energy is supplied externally to the gas before expansion. A possible method of generating hot jets is using energy released in a chemical reaction, as in liquid or solid propellant rocket motors. Both have the advantage of providing high energy per unit volume for propulsion simulators, and for creating gases (i.e., reaction products) under pressure available for expansion to form a jet. This subsection describes the liquid propellant concept. Solid propellant gas generators are described in Subsection 4.2.4.

A wealth of information on liquid propellant motors is available in the literature.[3] The motors are generally classified into two types: mono-

propellant, which uses a single chemical compound; and bipropellant, which uses two compounds. In the latter, a fuel and an oxidizer are mixed to produce energy via a chemical reaction. For a monopropellant, a catalyst is generally used to decompose it and release chemical energy. Monopropellants have the advantage that tankage, ducting, and pumping devices are required only for one liquid. Therefore, monopropellant motors are lighter, more compact, mechanically less complex, and operationally more reliable than bipropellant motors. The major advantage of liquid bipropellant motors over monopropellants is their ability to produce much higher specific impulses (300 to 400s versus 100 to 150s.).

In the current application to propulsive gas generation on MSBS wind tunnel models, liquid monopropellants are the most suitable for reasons of mechanical simplicity and compactness. Of the available monopropellants[XX] most are highly unstable, toxic, and a detonation hazard (nitromethane and nitroglycerine, for example). One candidate monopropellant, however, which can be used safely with simple precautions, is hydrogen peroxide (H_2O_2). Liquid H_2O_2 can be catalytically decomposed into steam and oxygen by the following reaction

$$H_2O_2(\ell) \xrightleftharpoons[\text{catalyst}]{} H_2O(g) + \frac{1}{2} O_2(g) \quad . \tag{13}$$

Some effective catalysts are pure silver metal, samariam oxide (Sm_2O_3) coated silver and sodium permanganate (Na_2MnO_4). For 100 percent pure H_2O_2, the equilibrium reaction temperature is 1250°K, with a specific impulse of approximately 146s for a 20:1 pressure ratio nozzle.

Hydrogen peroxide has significant advantages as an on-board propellant for wind tunnel models. Table 4 contains relevant physical and chemical properties of H_2O_2. In high concentrations, it has a high density (1.3 g/cm^3) which enables storage of relatively large mass of H_2O_2 in a given volume. The products of decomposition, steam and oxygen are clean (i.e., particle-free)

Table 4. Physical Properties of Hydrogen Peroxide*

Chemical formula	H_2O_2
Molecular weight	34
Color	Colorless
Odor	Slightly acidic
Solubility	Miscible with water in all proportions
Density	1.3 g/cm^3
Boiling point	126°C
Freezing point	-40°C
Vapor pressure at 30°C	10.1 mm Hg

*70% concentration by weight in a water solution. This is equivalent to a volume strength of 300 which is the volume of O_2 released per unit volume of the solution.

and non-toxic. Although not intended in the present application, the oxygen can be used as oxidizer for burning additional fuel, such as a hydrocarbon. The low reaction temperatures during decomposition ease cooling problems and result in longer operational life. An important consideration for H_2O_2 is that it is inexpensive, e.g., less than $10 per pound. Finally, H_2O_2 is a stable compound and decomposes very slowly unless contaminated by catalytic impurities. Its stability (i.e., negligible possibility of detonation) coupled with low freezing point and high boiling point, permit storage of H_2O_2 under ordinary climatic conditions.

The only disadvantage of hydrogen peroxide, especially in high concentrations (required for producing steam rather than water), is the necessity of proper handling procedures. However, since it is a widely used industrial chemical, the handling procedures are well established and straightforward.[4] The common sense precautions recommended for its storage are also described in

Ref. 5. The primary consideration in handling and storage of H_2O_2 is the use of proper material (i.e., pure aluminum, aluminum alloy 5284, teflon, and pyrex glass) free of catalytic contaminants. Davis and Keefer[6] and Cleaver[5] contain further details of the equipment (valves, hoses, etc.) and handling precautions for hydrogen peroxide in high concentrations. An important consideration for storage is adequate venting to avoid buildup of pressure due to very slow release of O_2, and locating the storage containers away from combustible materials. Plenty of water should be available wherever H_2O_2 is stored or used, since it is an effective dilutant and antidote for skin contact with the peroxide.

The use of hydrogen peroxide in thrust-producing devices dates back to the German V-2 rockets and the Me-163 rocket airplanes. Sanz[7] describes a hobbyist's simple design of a hydrogen peroxide rocket motor. The technology of liquid monopropellant motors is proven and well-understood. During the Phase I feasibility study, a conceptual design of a H_2O_2 propulsion simulation for application in MSBS wind tunnels was developed. Figure 8 shows the design

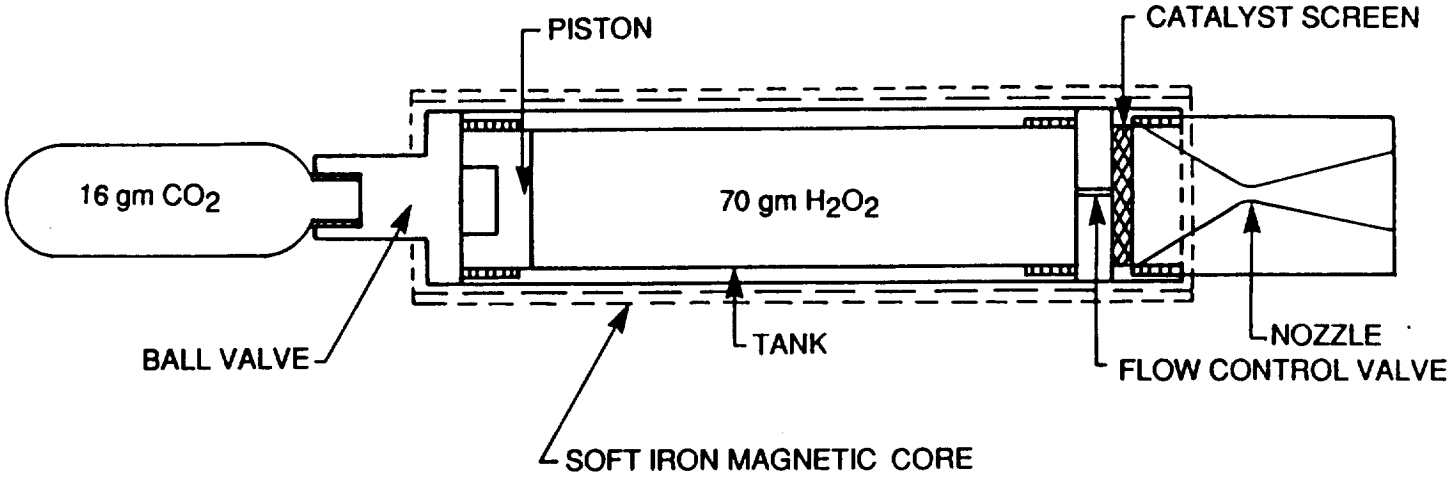

Figure 8. Conceptual Design of a Liquid Monopropellant Propulsive Jet Simulator

sized for approximately 4s thrust duration with an envelope of about 12 in. long and 1.25 in. diameter. The design can be easily scaled to larger sizes compatible with wind tunnel models. Table 5 lists the design parameters scaled from Ref. 7 for a 5-lb thrust, 4s duration motor A design which is specific to requirements of Eq. (12) will have to be developed through experimentation in Phase II.

The basic elements of a hydrogen peroxide propulsion simulator are: a tank for holding the liquid monopropellant and a device to pressurize it, a catalyst pack through which the liquid flows and decomposes into oxygen and steam, and a nozzle (which can be a simple orifice) to expand the gaseous products. In the proposed design, the pressurization of the peroxide is achieved by means of an expansion of liquidifed CO_2 acting against a piston inside the H_2O_2 tank. The idea of the CO_2 cartridge is the same as in the compressed gas concept described in Subsection 4.2.2. There are two valves, a ball valve which directs the CO_2 from the tank to the piston and a flow control valve which turns the liquid hydrogen peroxide flow on/off and controls the flow rate. The control valve is a solenoid which can be remotely operated. The ball valve is screwed on to the threads of the CO_2 cartridge

Table 5. Typical Design Parameters* for Hydrogen Peroxide Propulsion Simulator

Thrust	5 lb
Duration	4s
Chamber pressure	400 psia
H_2O_2 weight	0.16 lb
H_2O_2/CO_2 weight ratio	18.5:1
Nozzle throat area	0.0125 $in.^2$ (1/8 in. diam)
H_2O_2 flow control orifice	0.0015 $in.^2$ (0.044 in. diam)
Approximate weight	0.5 lb

*Scaled from Ref. 7.

through a cap-piercing fitting. This enables the liquid CO_2 to act on the piston when the ball valve is opened prior to a wind tunnel run. As the liquefied CO_2 vaporizes, it maintains a constant pressure on the piston until all the liquid has changed phase. The maintenance of constant pressure is an important design consideration since it determines the flow rate through the control valve. The latter can be a simple orifice, if only a single thrust interval is desired from the motor. The design in Figure 8 features a threaded, changeable expansion nozzle. The pressure of combustion products in the reaction chamber can be controlled by controlling the liquid H_2O_2 flow through the orifice. This can be done by varying orifice size.

The important issues in the design of hydrogen peroxide propulsive gas generator are: 1) materials of various components; 2) materials and structure of the catalyst pack; 3) H_2O_2 operating conditions; and 4) safety considerations. These are discussed in some detail below.

1. Materials for Components

The material for the tank in Figure 8 can be pure aluminum or alloy 5284. In that case the entire assembly must be fitted inside a annular soft iron core for magnetic suspension application, as shown by dashed lines in Figure 8. A very attractive alternative to the aluminum tank is a teflon-coated iron pipe, which serves as part of the magnetic core. Teflon is a qualified storage material for hydrogen peroxide, as mentioned earlier. The materials for valves and orifice/tubing can be aluminum alloy or stainless steel type 304 or 316. Stainless steel is designed as Class 2 material for limited-contact use with H_2O_2.[6] Aluminum and teflon designated as Class 1 materials for long-term use. Since the propulsion simulator is expected to be operated intermittently and to be purged with an inert gas afterward, the use of stainless steel in some components should not present any problems. The seals around the piston disk in Figure 8 should be braided teflon. A satisfactory lubricant for H_2O_2 equipment is fluorolube grease.[6]

2. Catalyst Pack

A principal component of the H_2O_2 propulsion simulator is the catalyst pack. While variety of solid (such as silver, cobalt, or copper) and liquid (sodium or potassium permanganute) catalysts with various efficiencies can be used to decompose hydrogen peroxide according to the reaction in Eq. (13), the compactness and simplicity requirements of the wind tunnel application points to a solid catalysts. Scatterfield and Sarda[8] have investigated effectiveness of various metals for liquid H_2O_2 decomposition. They found silver to be more effective (measured in terms of rate of oxygen production) than any other metal by two orders of magnitude, and thus it is an obvious choice for the catalyst. The design of catalyst packs has been studied in detail by Noah and McCormick.[9] These investigators have recommended metallic silver coated with samarium oxide (Sm_2O_3). The mechanism of decomposition is as follows. As liquid hydrogen peroxide passes over and around the wires in the catalyst pack, silver ions pass into the H_2O_2 solution and react with the H_2O_2 molecule decomposing it into oxygen and water vapor. The reaction is exothermic, increasing the temperature of the catalyst screen and the peroxide. This in turn causes the reaction rate to increase further in a matter of milliseconds until the equilibrium temperature of the reaction is reached. The equilibrium reaction rate continues indefinitely unless the catalyst is poisoned by contaminants.

Important parameters for design of the catalyst pack are its surface area, compression, and depth. The greater the surface area, larger the heat release, and shorter is the time required to reach equilibrium reaction rate. The result is a shorter starting transient for the propulsion simulator. Increased compression of the pack causes the liquid to follow a more tortuous path through the catalysts and thus increases its residence time. In turn, this increases the heat conducted to the catalyst and the propellant, again reducing the starting transient. Increase in the depth of the pack ensures that liquid H_2O_2 has completely decomposed into gaseous products and no liquid escapes from the nozzle. This aspect is especially important when the simulator is to be started with both the catalyst and the peroxide are at low

or ambient temperature, as would be the case in wind tunnel applications. Given the limitations on the mass carried on board the simulator and the need to avoid splashing on wind tunnel hardware, make it necessary that no liquid H_2O_2 leaves the nozzle.

An important consideration pertinent to the design in Figure 8 is that the CO_2 gas cannot be allowed to contact the catalyst sources as it poisons and deactivates silver (or silver coated with samarium oxide). Therefore, the piston between the CO_2 and H_2O_2 chamber must be properly sealed. Furthermore, any teflon threads or fluorolube grease should not enter the catalyst chamber as these materials are likely to ignite at reaction temperature and cause hot spots and melting of the metal in the pack.

The discussion above shows that proper catalyst pack design is critical to the adequate functioning and operating life of a hydrogen peroxide propulsion simulator. This design activity will form an important part of Phase II effort.

3. H_2O_2 Operating Condition

The concentration, temperature, and pressure of the liquid hydrogen peroxide have considerable effect on the temperature of decomposition products and transient characteristics of the simulator. Therefore, proper choice of these parameters is very important in MSBS wind tunnel applications. The concentration and temperature of H_2O_2 determines the temperature of the products of decomposition and hence the exhaust jet temperature. Figure 9, taken from Ref. 8, shows this dependence. For 90 percent concentration by weight of hydrogen peroxide, which can be procured relatively easily, and room temperature (70°F) operation of the motor, a jet with stagnation temperature of approximately 1370°F (1000°K) will result. At lower concentrations, lower jet temperature can be obtained. Thus, concentration of H_2O_2 is a useful parameter to vary as long as the H_2O in Eq. (13) exists as vapor, because formation, accumulation,and eventual ejection of liquid water from a propulsion simulator is not desirable.

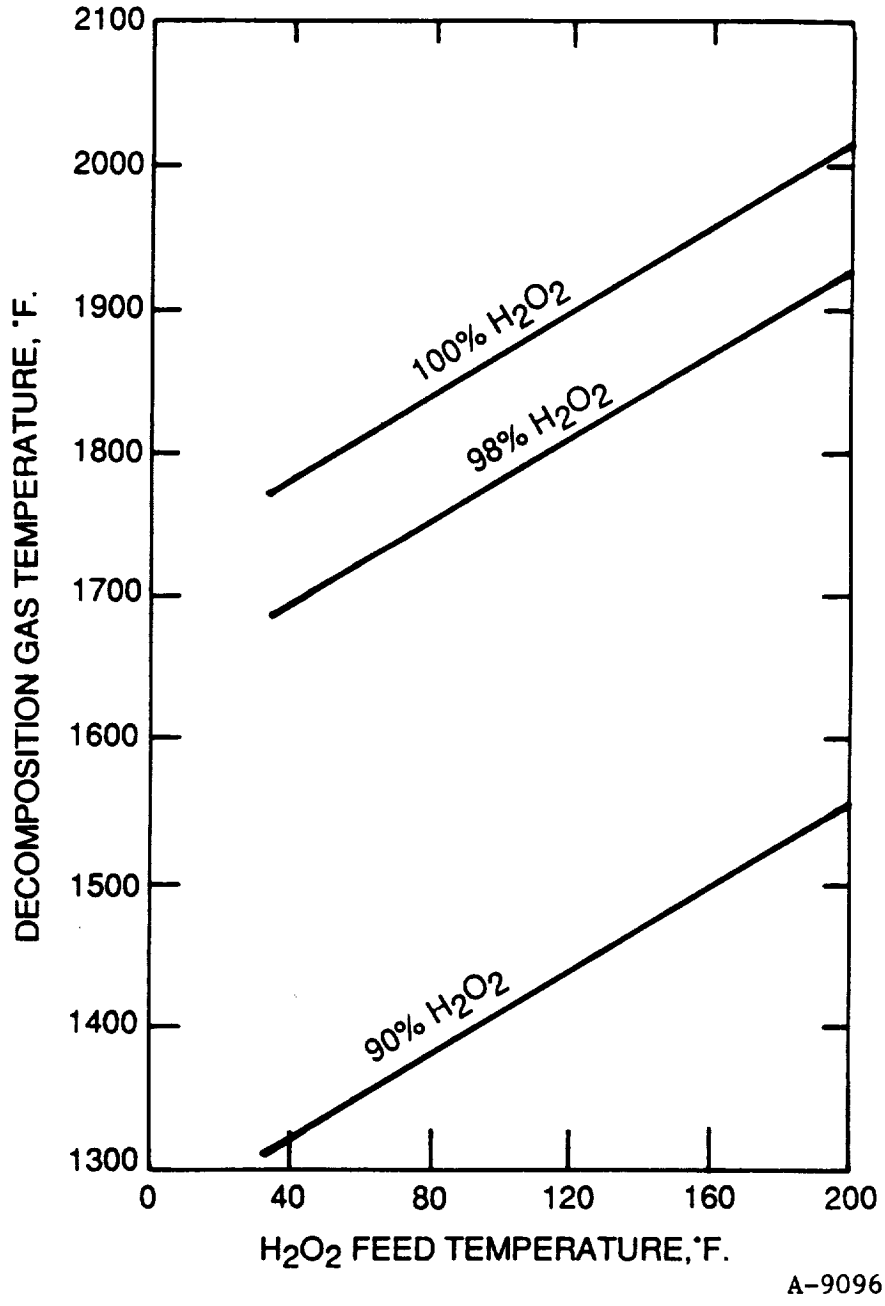

Figure 9. Effect of Liquid Hydrogen Peroxide Temperature on Final Reaction Temperature for Various Concentrations by Weight. Chamber pressure = 300 psia (Ref. 9).

The effect of hydrogen peroxide concentration on decomposition rate, expressed equivalently in terms of the rate of O_2 production per unit area of silver catalyst, is shown in Figure 10 adapted from Ref. 8. The decomposition rate appears to exhibit a maximum around 40 percent H_2O_2 concentration. Reference 8 does not give a physical explanation for this phenomena. It is clear from the last two paragraphs that the effect of systematic variation of H_2O_2 concentration on propulsion simulator performance should be an important part of the Phase II investigation.

The pressure of the catalyst or reaction chamber also influences the reaction rate, as one might expect. Higher the pressure, higher the steady-state reaction rate and shorter the time required to approach steady state.[XX]

The concentration, temperature, and pressure of the hydrogen peroxide not only affect the steady-state characteristics of the decomposition reaction but also its transient characteristics. The latter determine the starting/ stopping (i.e., on/off). characteristics of the propulsion simulator. This is of particular relevance to the MSBS applications. The MSBS control system must respond sufficiently fast to prevent the movement of the wind tunnel model due to impulsive axial (i.e., thrust) forces as the propulsion simulator is turned on or off. Figure 11a and 11b illustrate experimentally measured starting transient for H_2O_2 feed temperatures of 80° and 35°F respectively for a particular catalyst pack design of Ref. 9. In the figures the transient time is defined as the point at which the chamber pressure first reaches the designed value, i.e., the slight overshoot is ignored. At the lower temperature of 350°F, the starting transient time of 208 ms is significantly higher than the 122 ms at 80°F, for 90 percent concentrated hydrogen peroxide. Based on Figure 10, one would expect the starting transient to be a strong function of concentration, although no measurements are available in the literature. A motor based on a catalyst pack design, which was different from that for which the data in Figure 11 were obtained, was also built and tested by Davis and McCormick.[9] They measured starting and stopping transients are shown in

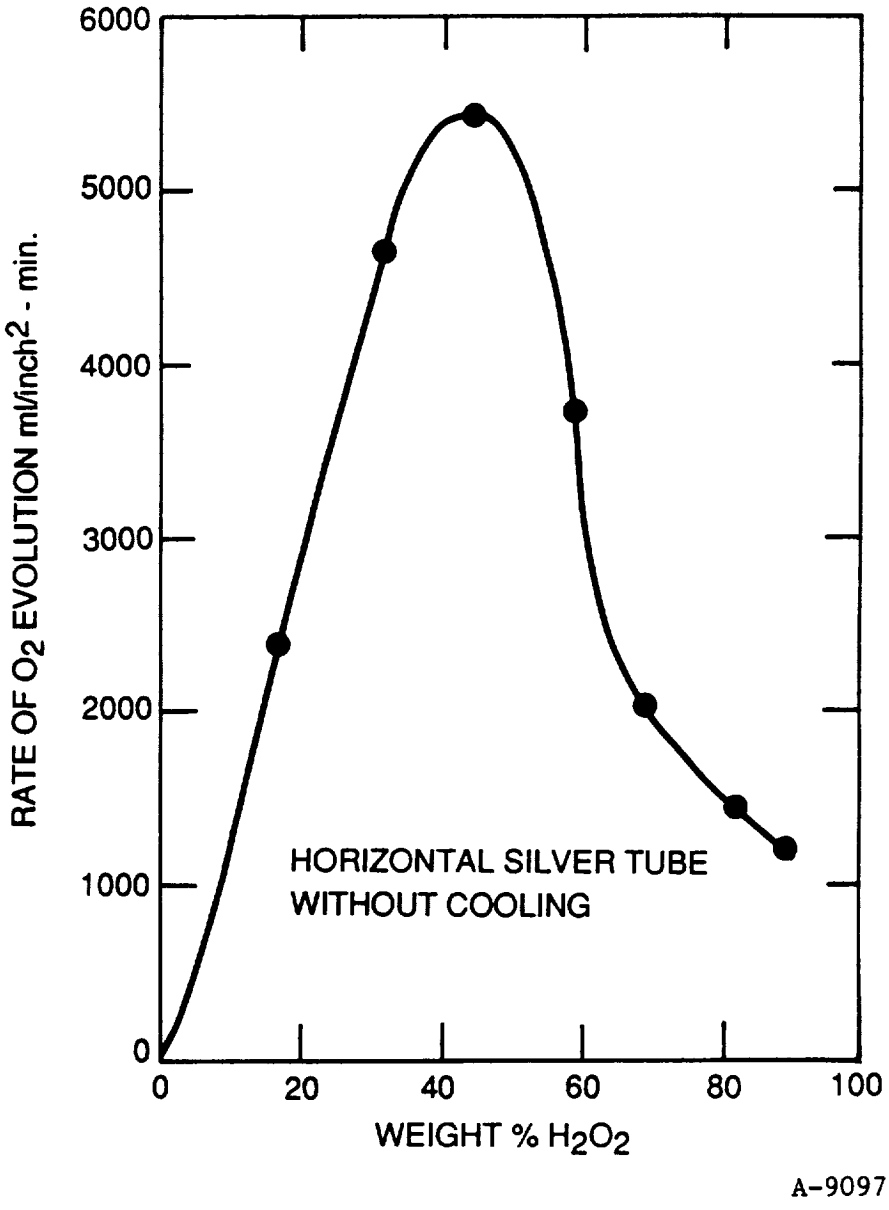

Figure 10. Hydrogen Peroxide Decomposition Rate as a Function of Concentration at 30°C (Ref. 8)

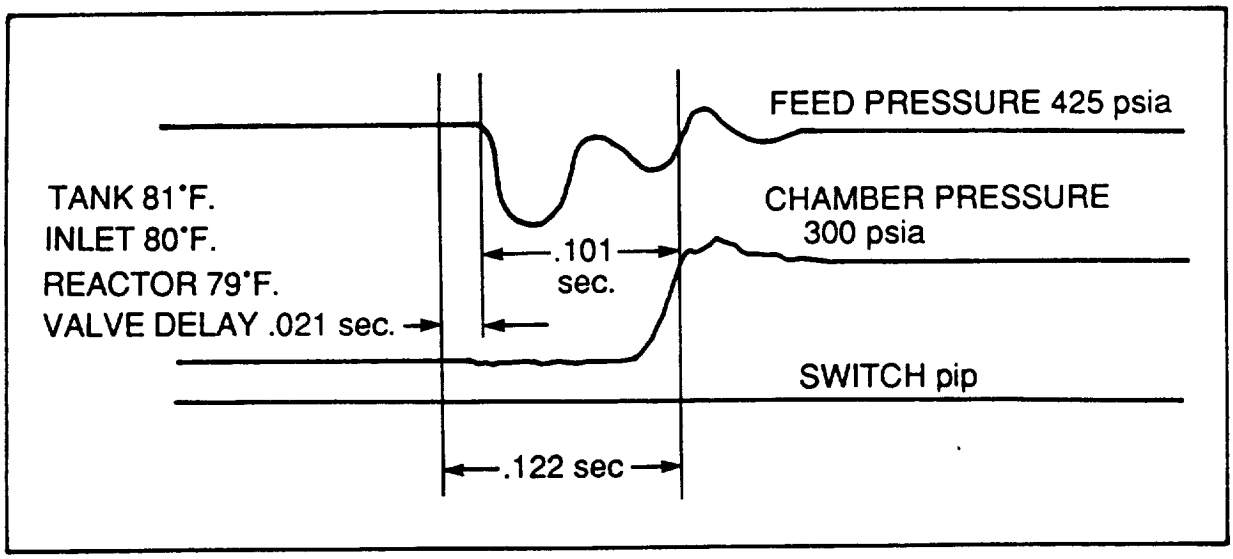

(a) H_2O_2 Temperature = 80°F

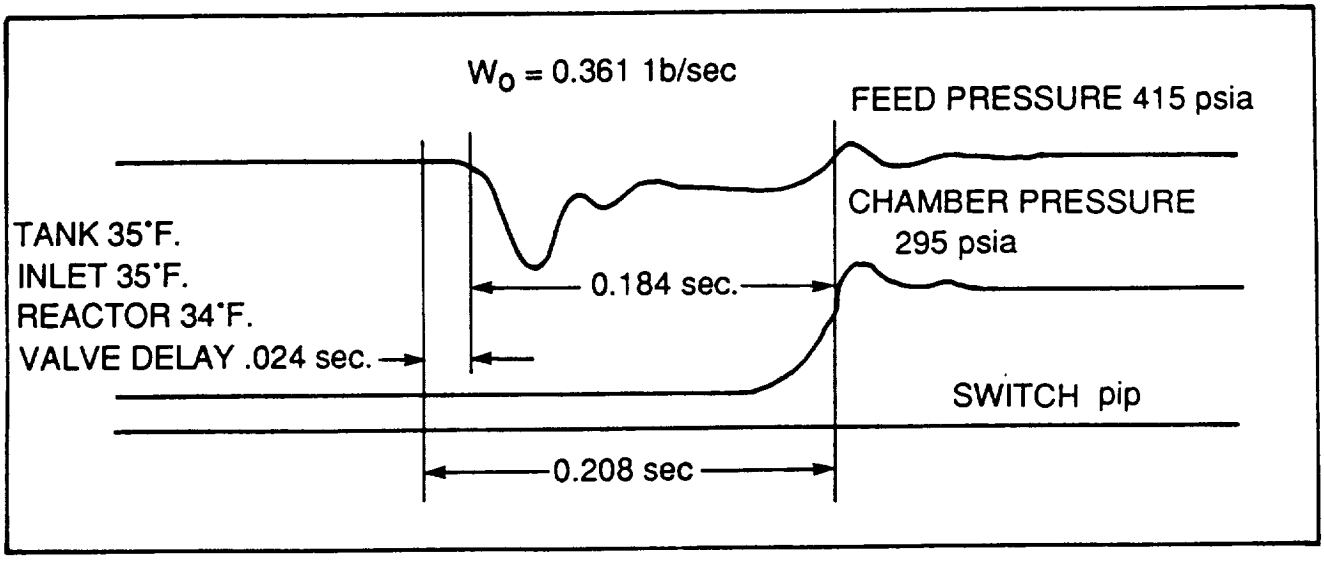

(b) H_2O_2 Temperature = 35°F

Figure 11. Starting Transient for a Typical Silver Catalysts Pack as a Function of Liquid H_2O_2 Temperature (Ref. 9), 90% H_2O_2

Figure 12. Note that apart from the catalyst pack, the H_2O_2 operating temperature for Figure 12 was different (50° to 70°F) from that of Figure 11 (81°F). The motor thrust (24 lb) and chamber pressure were the same in both cases.

4. Safety Considerations

The use of high strength (> 80% by weight) hydrogen peroxide requires certain well-established and straightforward storage and handling procedures,[4] as explained in the beginning of Subsection 4.2.3. Additionally, proper safety features must be designed into the H_2O_2 propulsion simulator for wind tunnel applications. These include a relief valve on the H_2O_2 storage tank (Figure 8) to avoid dangerous pressure buildup due to any reason. The design must avoid accumulation of liquid H_2O_2 anywhere in the system, which can later decompose uncontrolled and unattended by experimenters. This can be achieved by a wash (with distilled water) and purge (with dry N_2) procedure after a series of tests with the simulator has been completed. Prior to using the simulator for the first time or after long shelf storage, the hardware must be

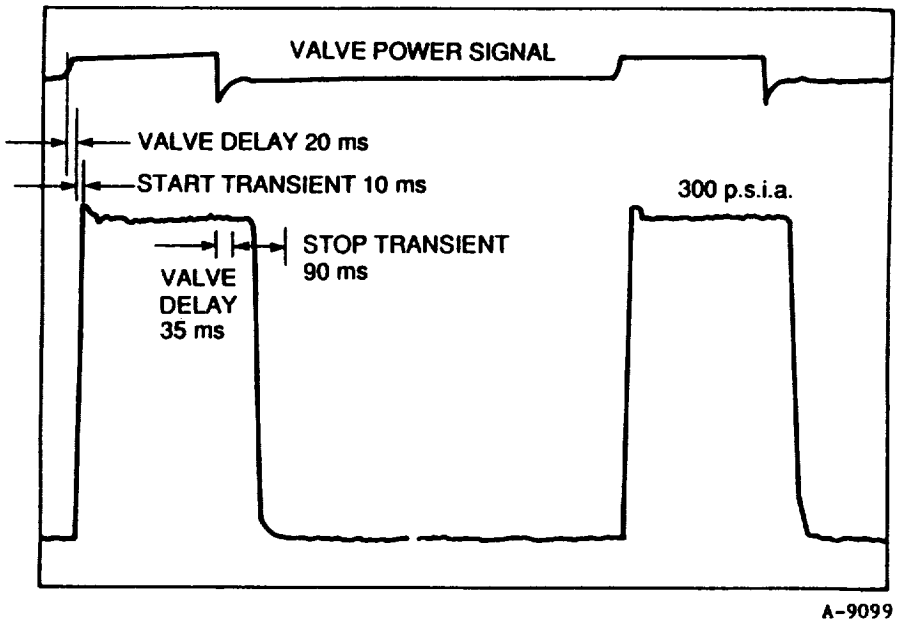

Figure 12. Starting and Stopping Transient for a 24 lb, 90% H_2O_2 Motor with Silver Catalyst Pack (design different from that used for Figure 11 data). H_2O_2 temperature range 50° to 70°F.

thoroughly passivated to ensure maximum peroxide stability. This involves a series of washing with a detergent solution to remove oils etc., then distilled water to remove the contaminated detergent solution, followed by weak acid solution (sulfuric, nitric, or phosporic) and finally with distilled water. The equipment in Figure 8 must be designed to accomplish the various passivating procedures. As mentioned earlier, the catalyst packs must be designed properly to make sure than no peroxide is expelled from the nozzle during the starting transient and minimal liquid water is released during the shut down transient. Also, venting must be provided in the design as necessary during the time the simulator is in the wind tunnel in a standby mode.

4.2.4 Solid Propellant Gas Generator

Like the liquid monopropellant propulsion simulator just described, a solid propellant gas generator can be used to obtain hot jets at moderate mass flow rates of 10 to 50 g/s, and burn times of the order of 5s can be easily achieved. The technology of miniature solid rocket motors is very mature.[10] Solid rockets with precise tailoring of thrust versus time can be designed and even the exhaust characteristics can be specified to a degree. Solid rockets are, of course, more compact than liquid rockets while achieving similar or higher specific impulses. The compactness results from the fact that the propellant (fuel plus oxidizer) has a higher density (1.6 to 1.7 g/cm^3) and does not require pressurization devices or valves like the liquid propellant system.

The main disadvantage of a solid propellant propulsion simulator is that the jet cannot be stopped and restarted, short of introducing very complex grain and ignition designs. Thus, each burn requires replacement of the propellant cartridge. Since each cartridge contains a carefully designed and fabricated grain, it is expensive (of the order of $100). Therefore, in wind tunnel applications requiring repeated firing of the propulsion simulator, the solid propellant approach is likely to be expensive. Another potential disadvantage of this approach is that the exhaust may contain particulates and corrosive chemicals which can deposit or tunnel hardware. This problem obviously does not arise in open circuit tunnels, such as the NASA Langley and the

University of Southampton MSBS facilities. Even in close circuit tunnels, operating at room temperatures (as opposed to cryogenic), the exhaust (~ 40 g/s) will be quickly diluted by the free stream of much higher mass flow rate (> 2 kg/s). Furthermore, as will be seen later in this subsection, it is possible to tailor propellant composition to minimize the particulate exhaust. Another concern, typical of solid rockets, is one of ignition of the grain, which must be achieved remotely for MSBS applications. It appears to be an easily soluble problem through remote ignition by a squib, which receives power from a small on-board battery pack. The arrangement will be similar to that in Figure 7, where a laser-activated switch is used to close a battery circuit.

To investigate the feasibility of a solid propellant gas generator as a propulsion simulator, Morton Thiokol, Inc. (MTI), Elkton Division, was consulted.[11] In addition to the general design requirements of Eq. (12), MTI set a goal of burn time equal to 3 to 5s; throat area of 0.14 $in.^2$ as discussed in Subsection 4.1.2, and particle-free, non-corrosive exhaust. They investigated various propellant formulations and grain geometry to achieve the design goals. Their results are discussed below.

Table 6 contains the composition and other properties of a solid propellant designated TP-N-3004, especially formulated as a minimum smoke propellant. It is a safe, stable composition based on ammonium nitrate. The composition of exhaust products is shown in Table 7.

Some basic aspects of the design of the propellant grain are described next. The relationship between burning surfaces area (A_s) for the solid propellant to throat area (A_t) is given by

$$\frac{A_s}{A_t} = \frac{P_c g}{R_b \rho c^*} \qquad (14)$$

where ρ is the propellant density, R_b is the burn rate, and c^* is the characteristic velocity. With the burn rate expressed as

Table 6. Composition and Properties of TP-N-3004 Propellant

Polymer, %	8.0
Plasticizer, %	22.0
Copper chromite, %	1.5
Boron, %	0
Ammonium nitrate %	68.50
Isp, s	227.3
Density, g/cm^3	1.609
Card gap test at 0 cards (detonation potential)	negative
Characteristic velocity, c^*, ft/s	4750
Strand Data	
r_{3500}, in./s	0.37
$\bar{n}$ (2 to 5 K)	0.69
TE-T-617 Data	
r_{3500}, in./s	0.40
$\bar{n}$	0.64

$$R_b = r\, P_c^{\bar{n}} \quad . \tag{15}$$

Expressions (14) and (15) can be combined as

$$\frac{A_s}{A_t} = \frac{g}{R_b r\, \rho c^*} \left(\frac{P_c}{C}\right)^{1-\bar{n}} \tag{16}$$

Table 7. Exhaust Products of TP-N-3004

Exhaust Product	Species Mole Fraction
CO (gas)	0.08129
CO_2 (gas)	0.12148
CR_2O_3 (solid)	0.00071
CU (gas)	0.00125
CU (liquid)	0.00016
H (gas)	0.00023
HO (gas)	0.00015
H_2 (gas)	0.07321
H_2O (gas)	0.49194
NO (gas)	0.00001
N_2 (gas)	0.22957
Condensables, % of mass	0.00509
T_{exit}, °F	4033
Mol. weight	22.9
Gas constant	2173 ft^2/s^2 °R
$\sqrt{RT_o}$	3193 ft/s

where C is a constant. Using values in Table 6,

$$\frac{A_s}{A_t} = 658.6 \left(\frac{P_c}{701}\right)^{0.35} \tag{17}$$

where P_c = chamber pressure expressed in psi. Equation (7) is plotted in Figure 13 with P_c expressed as a ratio with respect to ambient pressure (14.7 psia).

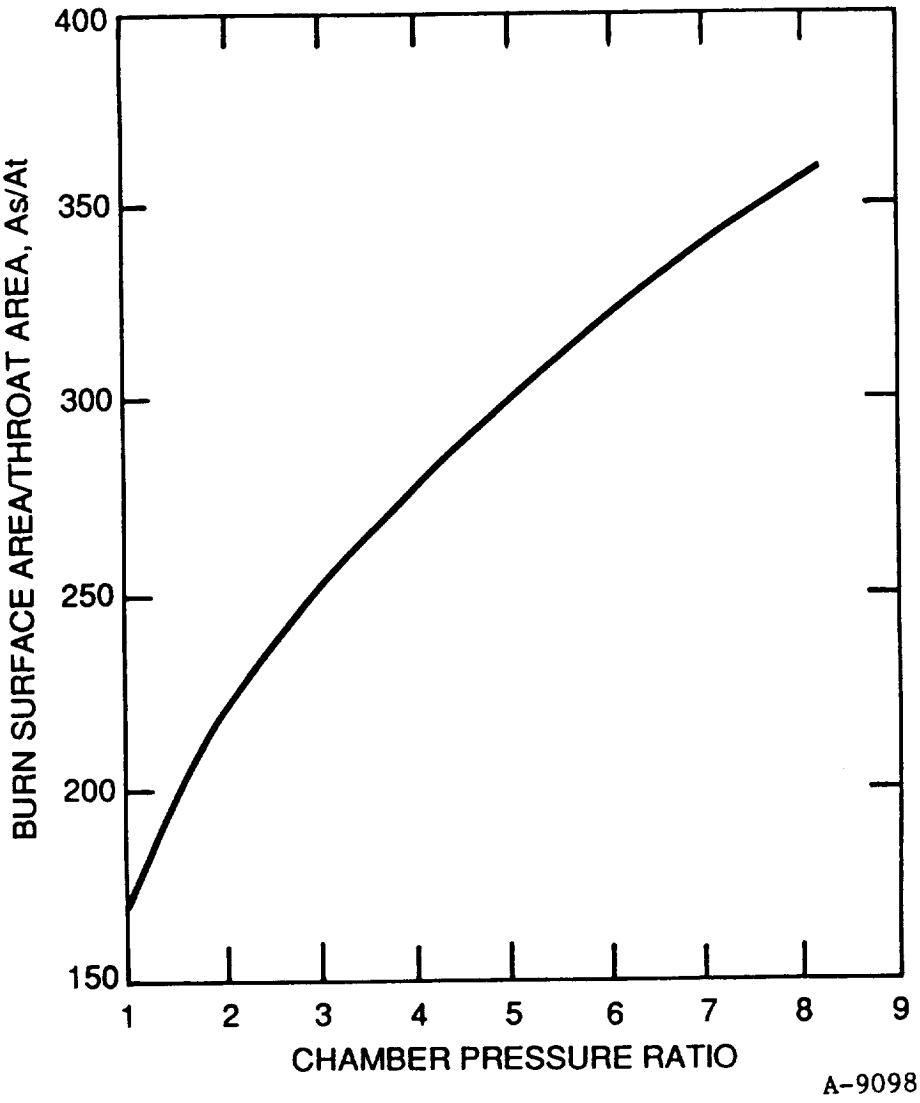

Figure 13. Burn Surface Area to Throat Area Ratio Versus Chamber Pressure for Solid Propellant Characteristics in Tables 6 and 7

Next, MTI investigated various grain geometries at representative pressures of 100 and 120 psia (other pressures could have been chosen). The resulting conceptual design is shown in Figure 14 and the motor characteristics are listed in Table 8. Although the range of parameters covered is outside of the range in Eq. (12), the results are generally consistent with Figure 4, i.e., mass flow rate per unit area. The thrust per unit area is

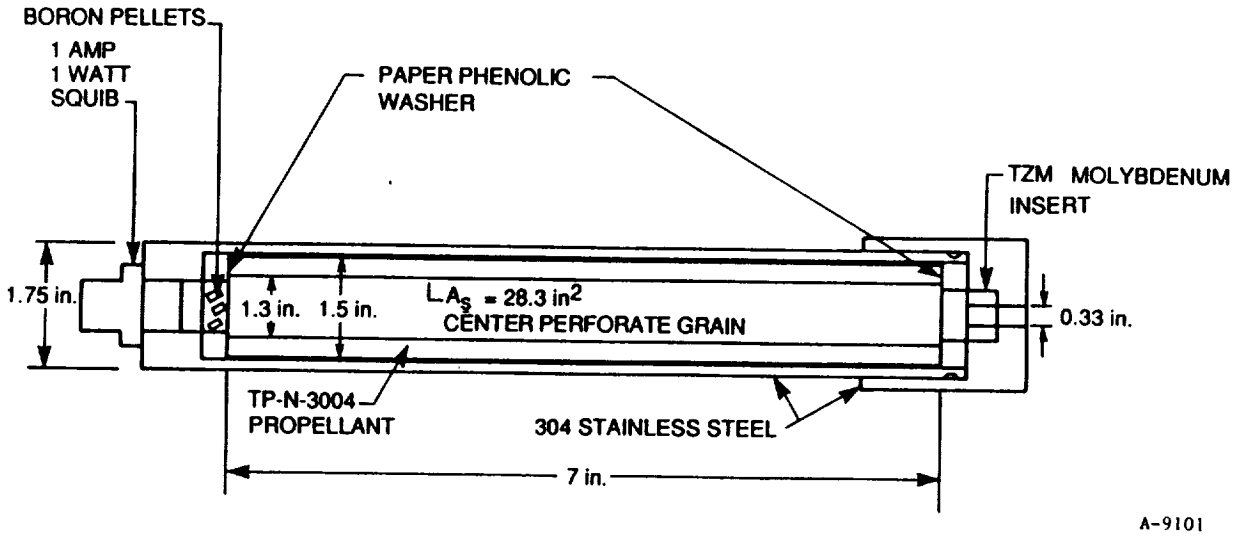

Figure 14. Conceptual Design of Solid Propellant Propulsion Simulation (courtesy Morton Thikol, Inc., Elktron Division)

low, however, when compared with Figure 5, the inconsistency appears to be at least partly due to the fact that the computation in Figures 4 and 5 assume ideal nozzle expansion to ambient pressure. In any event, the above exercise demonstrates that a solid propellant propulsion simulator with desired characteristics can be designed.

Further observation regarding the conceptual design of Figure 14 can also be made. The casing is a 304 stainless steel pressure vessel with a cartridge-type propellant loading system. It is possible to use magnetic material (to serve as MSBS core) in place of stainless steel. However, the effect of high temperatures in the chamber on the magnetics of the core is not clear, although MTI expects that the temperature of the motor assembly will be near ambient throughout the burn. The ignition scheme proposed in Figure 14

Table 8. Characteristics of Solid Propellant Motor Conceptual Design in Figure 14

Chamber pressure, psia (Pressure ratio)	~ 100 (6.8)
Chamber temperature	4493°R
Center perforate gain:	
- Surface area, A_s, in.^{2} - O.D. in./web thickness, in. - Length, in.	28.3 1.5/0.2 7.0
Throat area, A_t, in.^{2}	0.085
A_s/A_t	332.9
Thrust, F, lbf	5.75-7.5
F/A_t, lbf/in.^{2}	67-88
Mass flow, $\dot{m}$, lbm/s	0.061
$\dot{m}\sqrt{RT_o}/A_t$, lbm-ft/in.^{2}-s/s	2291

involves the usual electric squib acting on boron igniter pellets. Electrical power to the squib may be supplied externally by means of a thin wire (which carries negligible force) or with a battery/laser activated switch arrangement similar to Figure 7.

4.2.5 Laser-Assisted Propulsive Devices

Another potentially attractive and more innovative concept for propulsion simulation is that of laser-induced propulsion. The original idea of laser propulsion which involved beaming energy to a propulsion system with a high power laser was first proposed by Arthur Kantrowitz in the early 1970's.[12] The general concept involves using a remote laser beam to supply energy to a rocket to heat a chemically inert propellant.[13]

The thruster concepts considered have generally fallen into two categories depending on the type of laser waveform used: either continuous wave (CW) laser-heated thrusters or repetitively-pulsed (RP) laser-heated thrusters. Figures 15 and 16 depict respectively a CW and RP laser-heated thruster design. In the CW design, the power from a steady laser beam is used to heat a cold gas in the absorption chamber. The gas is then expanded through a nozzle to produce thrust. In the RP thruster design, power from a short pulse laser beam is used to create periodic "explosions" or detonations in a cold gas downstream of the throat, depositing the laser energy into the gas via laser-induced breakdown, followed by laser/plasma absorption. The resulting blast wave imparts a high velocity to the gas, creating thrust as it expands through the nozzle. Other RP thruster designs have used a repetitively-pulsed laser beam to directly vaporize a solid propellant and subsequently heat the propellant vapor further using a laser-supported detonation wave.[14]

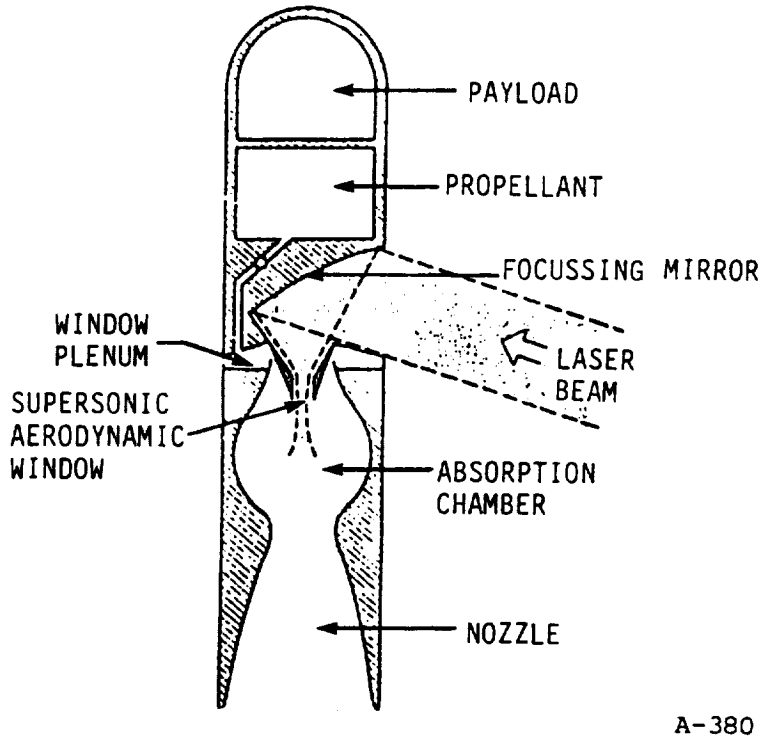

Figure 15. Schematic Diagram of a CW Laser Propulsion Concept

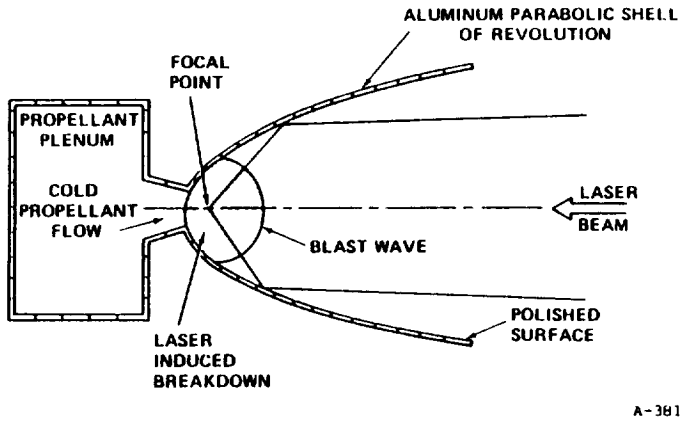

- PROPULSION SEQUENCE
  - COLD PROPELLANT FLOWS THROUGH THROAT
  - LASER ENERGY ABSORBED VIA INVERSE BREMSSTRAHLUNG DOWNSTREAM AT FOCUS
  - SHOCKED GAS EXPANDS OUT NOZZLE
  - SEQUENCE REPEATS: PROPELLANT USE CONTROLLED BY MASS FLOW AND LASER REPETITION RATE

Figure 16. Schematic of Repetitively-Pulsed Laser Propulsion Concept

The potential advantages of laser propulsion that have made it attractive for rocket propulsion are: 1) chemically inert propellants can be used; and 2) low molecular weight propellants can be heated to very high temperatures to produce high specific impulse. For the application to the simulation of air-breathing propulsion systems, high specific impulse (i.e., $I_{sp} \gtrsim 800s$) is not essential. Therefore, direct laser-induced evaporation of a solid surface (rather than ionization of a gaseous propellant) at normal vaporization temperatures should generally be adequate, provided specific impulses $\gtrsim$ 200s are not necessary.

For application to MSBS wind tunnels, laser propulsion has the following principal advantages: 1) the potential for localized generation of jets, such as high mass flow and low velocity lift jets, using laser-induced evaporation of pieces of solid materials located under the wing, fuselage, etc.; 2) simple, cheap,and inertia solids can be used as fuel; 3) the ability to turn the jet on and off and to modulate it by simply controlling the laser power reaching the propellant; and 4) the ability to vary the temperature and exhaust velocity of the jet by varying the incident laser flux. Laser propulsion also offers the interesting possibility of simulating the flow

through an inlet duct, prior to heating it remotely by a laser. In this case, however, the laser will be required to quickly heat the air flow seeded with a gas which absorbs the laser energy. The problem of heat transfer from the gases to the material of the model will also need serious considerations.

The advantage of laser-assisted generation of jets over the compressed gas and liquid monopropellant concepts is that no storage tanks, ducts, valves, etc., are required. Unlike the solid propellant concept, ignition mechanisms are not required. In contrast to both the liquid and solid propellant schemes, chemically-inert propellants can be used.

A major disadvantage of laser-assisted propulsion simulation is the large laser power required, even for the lowest thrust and mass flow rate levels. This aspect limits the applicability of the concept to MSBS wind tunnels, at least for small, diagnostic experimental facilities. The following discussion includes the issue of laser power.

The following three laser-assisted propulsion concepts were examined during Phase I.

1. Laser Ablation Thruster

The idea here is to vaporize an ablator material by energy of a laser beam, Figure 17a. Thrust results from ablator vaporization and momentum transfer to the surface as the material blows off. The thrust is given by

$$T = \dot{m} V_j \tag{18a}$$

with

$$\dot{m} = \frac{(1-R)\, P_L}{(H_v + C_p T_v)} \tag{18b}$$

where P_L = laser power, H_v = heat of vaporization, R = reflectivity of ablation, C_p = specific heat, and T_v = vaporization temperature, V_j = exit

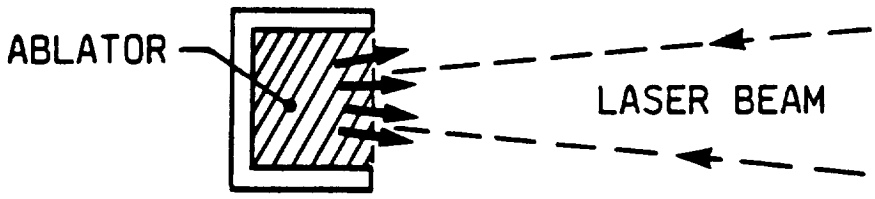

(a) Laser Ablation Thruster

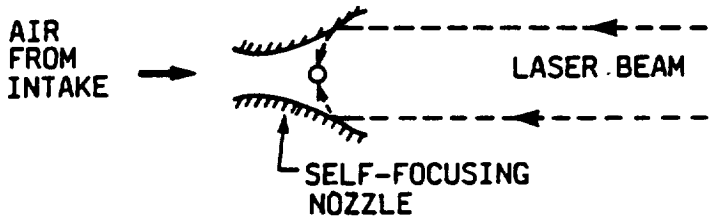

(b) Laser-Heated Air-Breathing Thruster

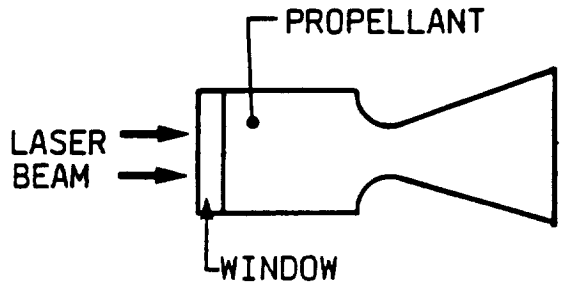

A-9094

(c) Laser-Augmented Conventional Thruster

Figure 17. Various Laser-Assisted Propulsion Concepts

velocity of jet, which is typically 4×10^4 to 1.2×10^5 cm/s for choked flow. For laser, one can define an impulse coupling coefficient as

$$C = \frac{\text{Impulse}}{\text{Laser Energy}}$$

$$= \frac{\text{Thrust x time}}{\text{Laser Energy}}$$

$$= \frac{T}{P_L} \quad . \tag{19a}$$

Another parameter of interest is the denominator $(H_v + C_p T_v)$ in Eq. (18b) which equals effective heat of ablation, Q^*

$$Q^* = \frac{\text{Laser Energy}}{\text{Mass Removed}}$$

$$= \frac{P_L}{\dot{m}} \quad . \tag{19b}$$

The laser power required then is

$$P_L = \frac{T}{C} \tag{20a}$$

and the resulting mass flow rate is

$$\dot{m} = \frac{P_L}{Q^*} \tag{20b}$$

which is the same as in Eq. (18b) when the ablator absorbs all the incident laser energy, i.e., reflectivity $R = 0$.

A large data base exists on the impulse coupling coefficient C and Q^* versus laser fluence for a variety of materials.[15] The fluence is defined as laser energy per unit area of the beam. Figures 18a and 18b show the variation of C and Q^* versus fluence for a number of inert materials for a single pulse of a repetitively-pulsed CO_2 laser (10.6 micron wavelength). These data were taken for materials ablating in vacuum.

It is seen that the coupling coefficient for typical materials is in the range of 1 to 20 dyne-s/Joule or 10^{-3} to 2 x 10^{-2} kg/kW. Thus, for a thrust requirement of 3 kg/cm^2 (Eq. 12b), the laser power, P_L from Eq. (20a) is in about 30 kW for a jet of 5 mm diameter. Assuming a low Q^* of 10 kJ/g from Figure 18b, the corresponding mass removal rate from Eq. (20b) is 3 g/s, which is very large for ablator materials currently under investigation.

Two new materials were evaluated experimentally during Phase I, and the results are discussed in Subsection 4.3.

2. Laser-Heated Air-Breathing Thruster

One of the potential advantages of this concept shown in Figure 17b is that it can, in principle, simulate an air intake. None of the other concepts considered thus far, compressed gas, liquid or solid propellant, offer this possibility. The idea in Figure 17b is that a laser beam focused at a point in the airstream achieves breakdown of air (plasma formation) and drives a detonation wave from that spot. This breakdown occurs in one laser pulse. The detonation wave causes creation of high temperature, high pressure gas behind it, which then expands through the nozzle to create thrust. The next pulse of the laser repeats the process. The concept is discussed in detail in References 16 and 17.

The most important advantages of this concept is that ambient air can be used as the fuel. The disadvantages include the need for surfaces to focus

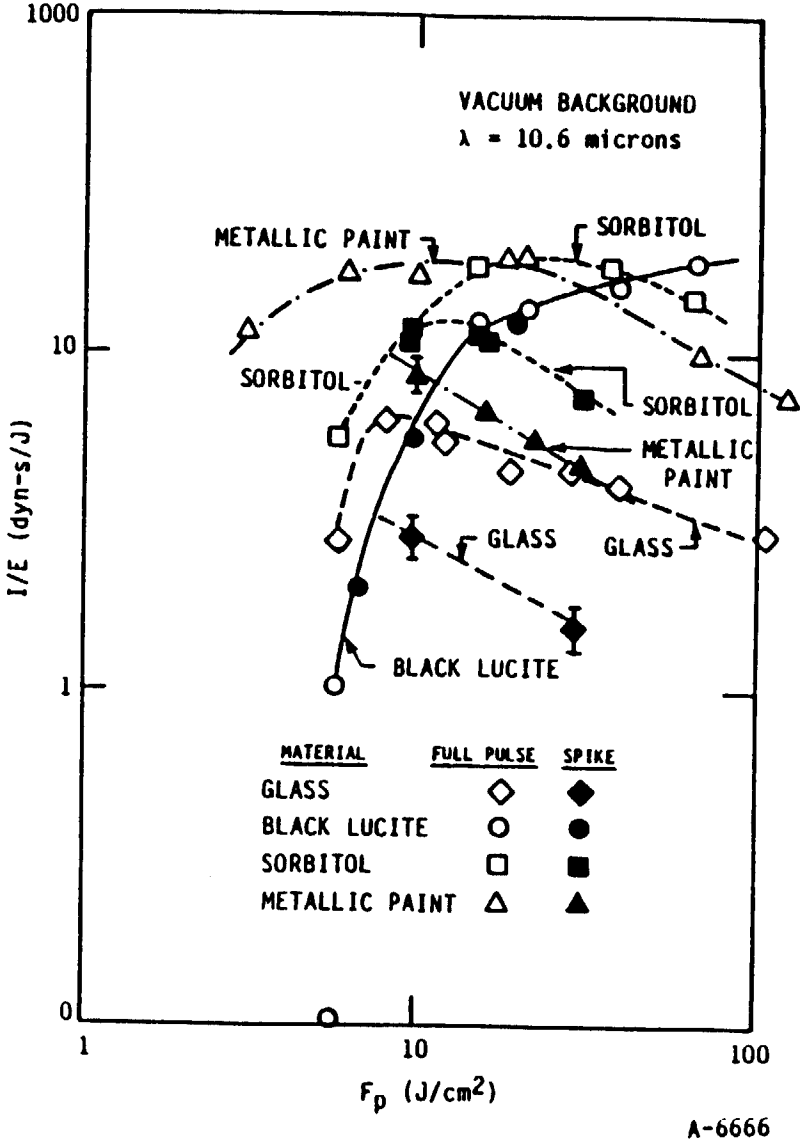

(a) Coupling Coefficient

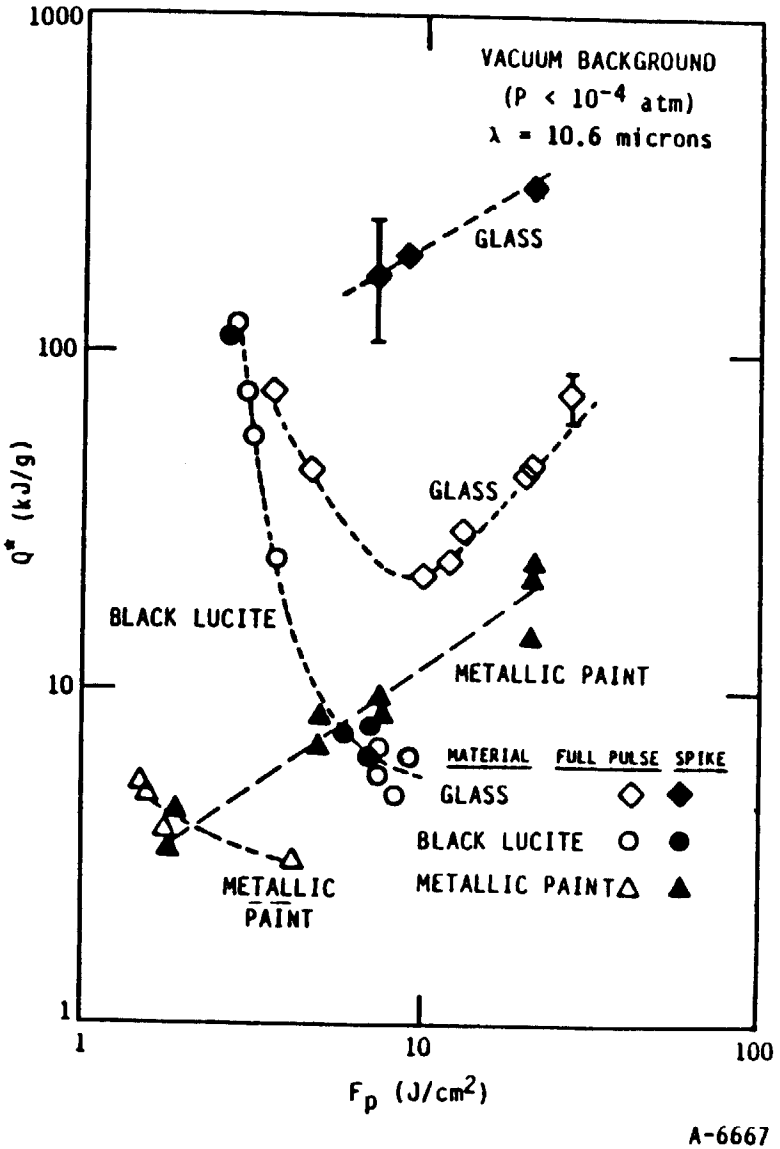

(b) Effective Heat of Vaporization

Figure 18. Impulse Coupling Coefficient and Effective Heat of Vaporization Versus Laser Fluence

the laser beam, a repetitively-pulsed laser which is commercially not available at very high power levels as opposed to a continuous wave laser. The average laser power required is 17 kW per Kg of thrust.

3. Laser-Augmented Conventional Thruster

As shown in Figure 17c, the idea here is to absorb laser energy directly into high pressure propellant vapor to elevate its stagnation temperature. The advantages are: a) that a conventional scheme for supply of the propellant (Figures 7 and 8) can be used with the laser largely used for additional heating; and b) a continuous wave laser can be used. The disadvantages are: a) fuel storage, valving complexities of conventional systems are retained; and b) propellant/fuel which absorbes laser energy efficiently is necessary. As an example, if ammonia (NH_3) were to be used in the compressed gas cylinder concept of Figure 7, a high power continuous wave CO_2 laser can be used for additional heating since it is known that NH_3 is a good absorber of the 10.6 micron wavelength.[18] The laser power required then depends on the absorption coefficient and the desired value of additional energy input to the propellant.

4.3 Diagnostic Experiments

The discussion in Subsection 4.2.4 reviewed the existing impulse coupling coefficient, C, and Q^* data for various materials. It was found that for the materials under consideration both C and Q^* were quite low, resulting in very high laser power required. Large laser power means expensive and bulky equipment occupying large space. During Phase I two potentially promising materials with low heat of vaporization were tested in PSI laboratory. The materials were Delrin and Ping-Pong, the latter in form of pieces cut from table tennis balls. Although the composition of Ping-Pong is not clear, it has distinct odor of camphor, which may explain its low heat of vaporization. The experimental apparatus and measurements are described next.

A Lumonics K103 Pulsed CO_2 TEA Laser was employed as the laser source in experimental diagnostics involving impulse and mass loss measurements of materials. It was operated in two distinct modes: a full energy mode of approximately 8 J with a pulse duration of about 2 μs, and a lower energy mode of about 2.4 J obtained with no N_2 in the gas mixture and consisting of only "gain-switched" spike of approximately 100 ns duration (FWHM). These energy values were confirmed by using a disc calorimeter to intercept the laser beam, which has been attenuated with plastic sheets of known transmission.

The sample materials considered for analysis were Ping-Pong and Delrin. These were cut into small square pieces of about 1.8 x 1.8 cm and taped onto sample mounts (1.9 x 1.9 cm piece with 1.27 cm hole) made from thin metal stock. The individual target sample was then mounted inside an evacuated stainless steel test chamber that was pumped to a pressure of less than 1.32×10^{-4} atm. The laser beam was directed toward the vacuum chamber by a beam directing mirror in front of the laser output coupler and concentrated onto the target by a barium fluoride lens, whose distance from the sample was adjusted to generate a spot size of about 0.082 cm^2. The resulting fluence (laser energy over spot area) thus ranged from about 3 to 30 J/cm^2 for the "gain-switch" spike and approximately 10 to 100 J/cm^2 for the full energy pulse, depending on the amount of beam attenuation.

For impulse measurements, the samples were mounted on a ballistic pendulum inside the vacuum chamber (Figure 19). The amount of laser-induced deflection, a quantity needed for impulse calculation, was obtained by directing a HeNe laser beam onto a metal in at the back of the pendulum and observing its displacement imaged onto a screen through a lens.

We have used the following equation to determine impulse:

$$I = (mx/M)(g/l)^{-1/2}$$

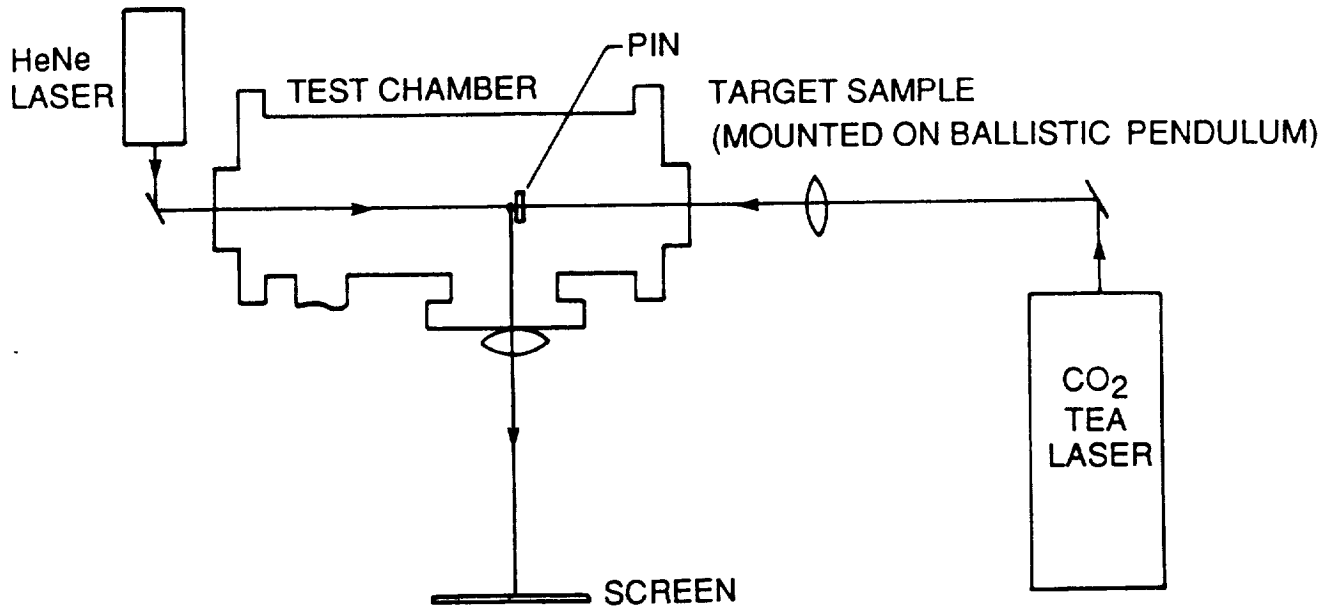

(a) Impulse Measurement

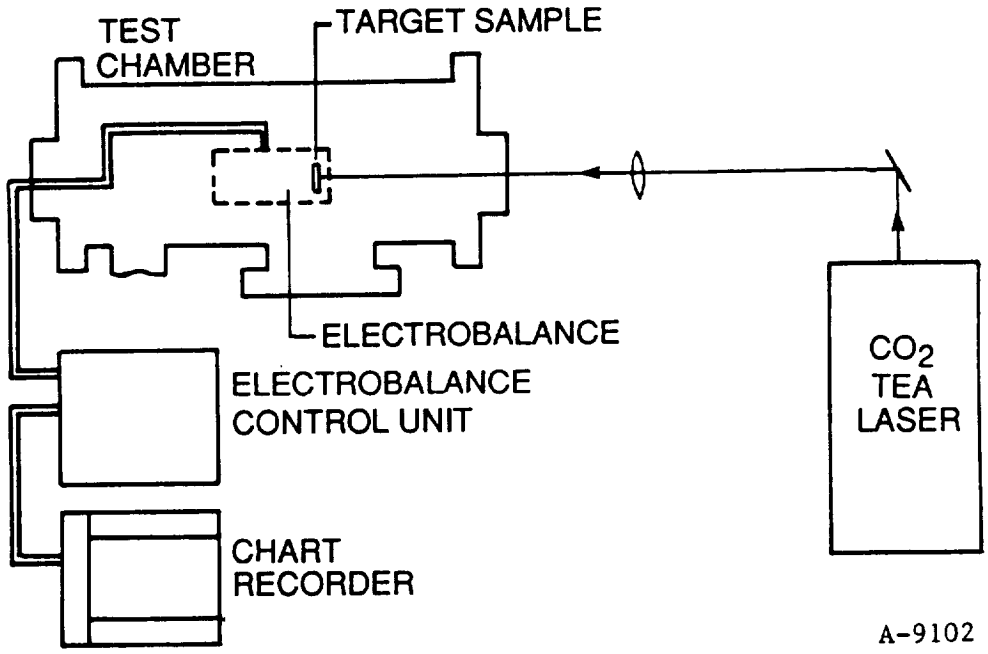

(b) In-Situ Mass Loss Measurement

Figure 19. Experiment Schematic for Laser-Induced Impulse and Mass Loss Measurement

where

I - impulse (dyn-s)
m - mass of sample and sample holder (gm)
x - half amplitude deflection (cm)
M - lens magnification factor: 5
g - gravitational constant: 980 cm/s^2
l - length of pendulum from pivot point to center of mass

and plotted the coupling coefficient, defined as impulse over incident laser energy, versus fluence.

To determine in-situ mass loss, a Cahn 2000 Electrobalance was used in conjunction with a Linear Chart Recorder (Figure 19b). With the sample placed in a target holder and mounted on loop A of the balance, and tare weights placed on loop B, one could adjust the electrical zero suppression to get a sufficiently sensitive scale for mass loss measurement. The amount of mass loss was then indicated by the change in the recorder trace and the Q^* (incident laser energy in kilojoules per gram mass removed) for the various materials was plotted against fluence.

The results from the above experiments are plotted in Figures 20 through 22. Figures 20a and 20b respectively show impulse coefficient C and effective heat of ablation Q^* versus laser fluence for Ping-Pong in vacuum. Comparing to the materials in Figure 18, the peak value of C is seen to be substantially higher (40 dyne-s/Joule or 0.04 kgf/kg) and Q^* is substantially lower (minimum value 2 kJ/g). Based on the measured value of C, the laser power required for Ping-Pong will be lower by at least a factor of 2. Figures 21a and 21b show C and Q^* data for 1 atm pressure. It is seen that the minimum Q^* value is about the same as in vacuum (2 kJ/g), but the peak impulse coefficient is lower by a factor of 4 under 1 atm. This means that for a given power level, the mass loss rate of the ablator is the same both under vacuum and 1 atm pressure, but the thrust is lower in atmosphere. The lower thrust at same mass loss rate means lower exit velocity for the ablator.

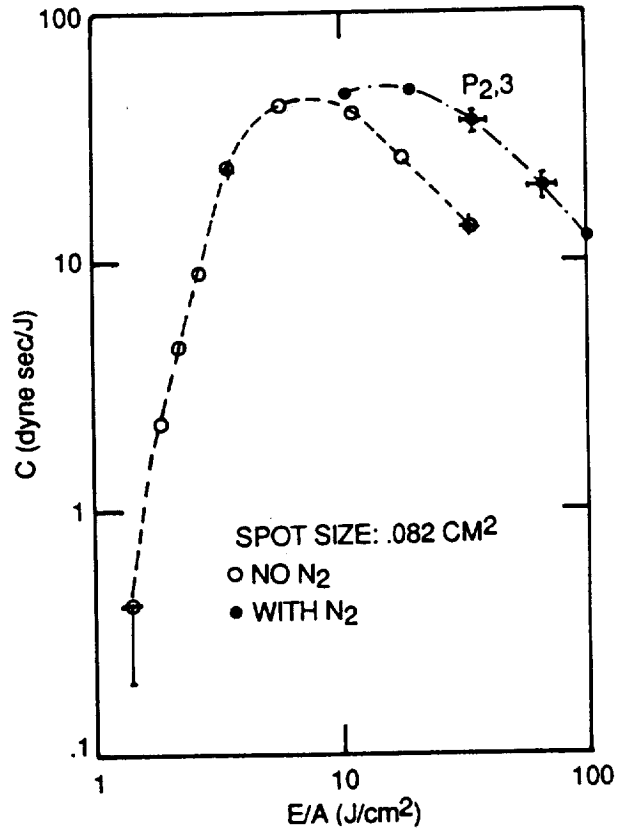

(a) Impulse Coupling Coefficient

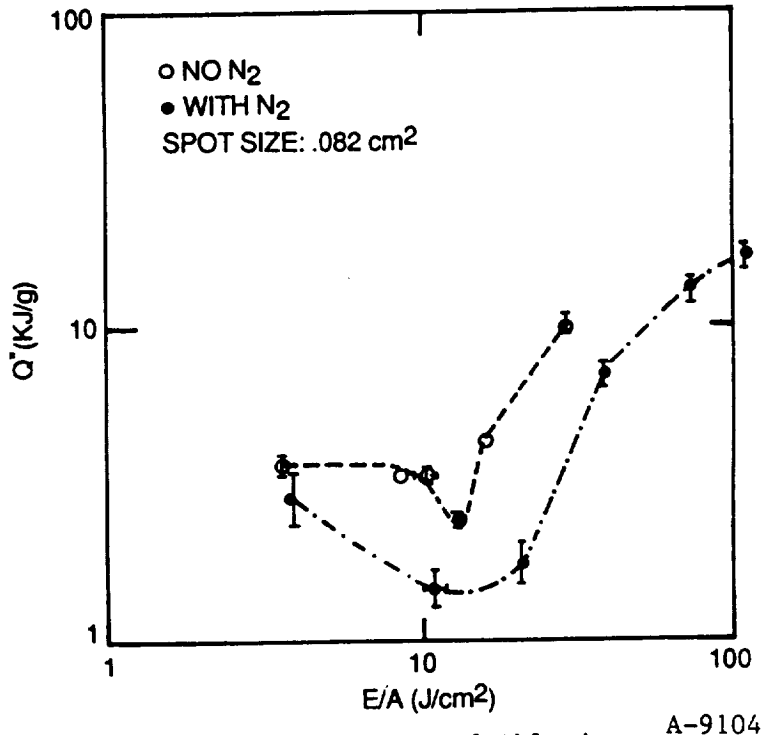

(b) Effective Heat of Ablation

Figure 20. Laser-Induced Impulse and Mass Loss Data for Ping-Pong Under Vacuum

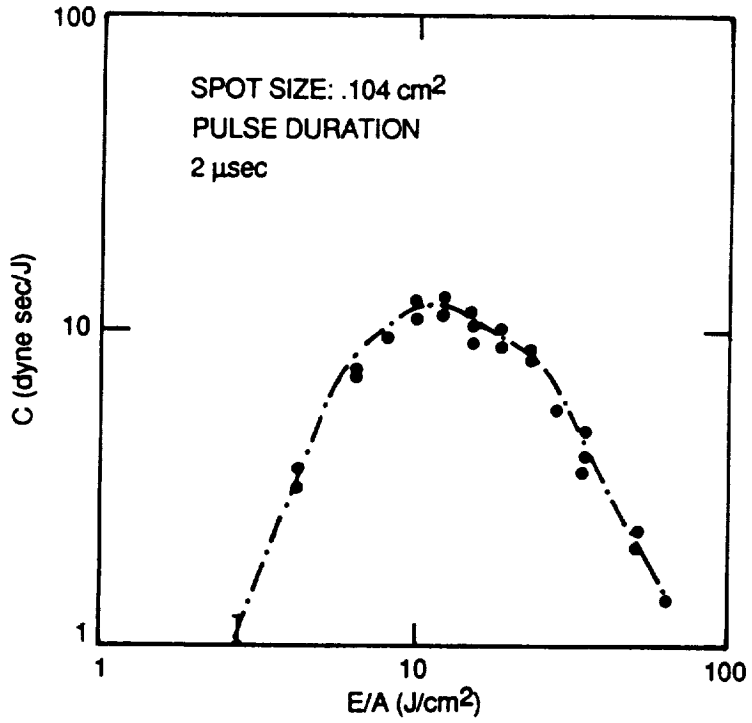

(a) Impulse Coupling Coefficient

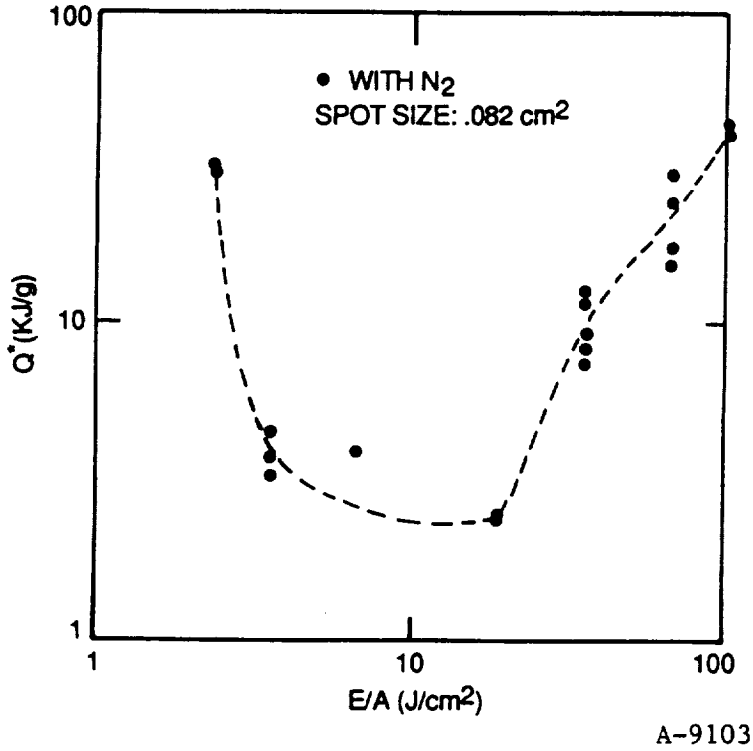

(b) Effective Heat of Ablation

Figure 21. Laser-Induced Impulse and Mass Loss Data for Ping-Pong Under 1 atm Pressure

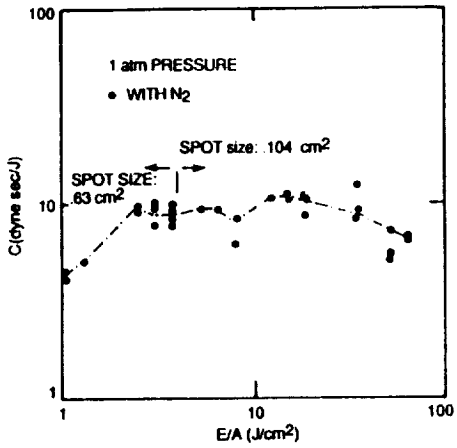

(a) Impulse Coupling Coefficient

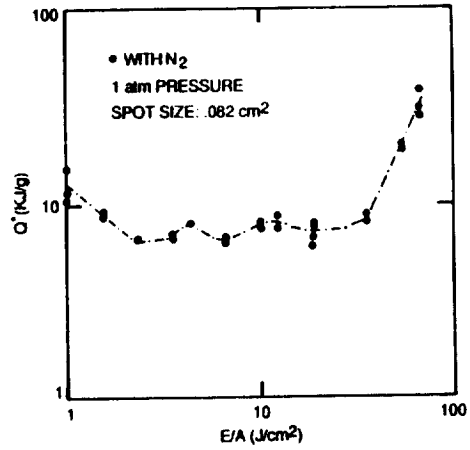

(b) Effective Heat of Ablation

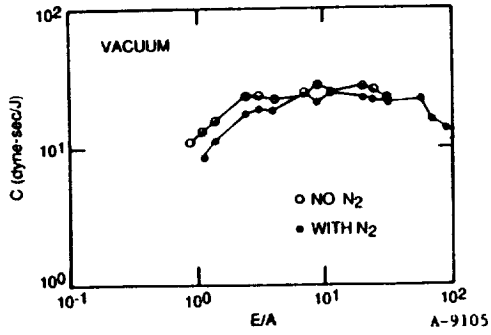

(c) Impulse Coupling Coefficient

Figure 22. Laser-Induced Impulse and Mass Loss Data for Delrin, 1 atm Pressure and Vaccum

Figures 22a and 22b show C and Q^* data for Delrin under 1 atm. Figure 22c shows corresponding data for C under vacuum from a separate experimental program at PSI. Q^* data under vacuum were not available. C and Q^* for Delrin do not exhibit a peak with respect to the pulse fluence. The value of C for Delrin is somewhat lower than that for Ping-Pong, but the Q^* is higher by a factor of 3-4. For these reasons, Delrin does not appear to be as promising an ablator as Ping-Pong for current application to on-board thrust generation for wind tunnel models.

The foregoing data point to the possibility of finding other materials with low Q^* and high C under atmospheric pressure. Further investigations need to be conducted in Phase II. It may be possible to find materials which are not inert but release chemical energy during laser irradiance, thus yielding high thrust at relatively low power.

4.4 Design of Propulsion Simulation Demonstrator Experiments

Thus far, the feasibility of various propulsion simulator concepts (Subsection 4.2) has been evaluated in light of the specification of exhaust jet characteristics (Subsection 4.1) and general integration requirements for MSBS wind tunnels (Subsection 4.2.1). One can now formulate a program for experimental demonstration of propulsion simulators in Phase II. For this purpose, it is useful to first rank the simulator concepts relative to each other in terms of applicable criteria as described below.

a. Ability to Meet Design Requirements

In Subsection 4.2 the ability of various propulsion simulator concepts to meet the design requirements of thrust, mass flow rate, and pressure ratio was discussed. The compressed CO_2 concept is limited primarily by the jet temperature (cold jet only). The liquid and solid propellant concepts can generate high temperature jets, but they may be limited to high pressure ratios necessary for maintaining high chemical reaction rates. Depending on

the power levels available, the laser-assisted propulsion concepts will be limited in thrust and mass flow.

b. Complexity of Design

Clearly, a simpler design is better in terms of reliability of operation, cost, etc. Laser concepts appear mechanically simpler compared to others.

c. Technology Maturity

The technology for solid and liquid propellant simulators is well-established. The compressed gas concept appears straightforward to implement.

d. Support Equipment Requirements

The laser concept needs a large laser with several kilowatts of power. These are bulky devices (including cooling systems) occupying hundred of cubic feet of space. The liquid hydrogen peroxide simulator requires proper filling and storage equipment for the monopropellant. It also requires nitrogen purge after a series of runs is complete. The solid propellant simulator concept involves storage of propellant cartridges in approved explosion-proof containers and some simple precautions. The compressed CO_2 concept requires minimal support equipment.

e. Compatibility With Wind Tunnel Models

The compressed CO_2 concept is compatible with small (< 1.5 in. diam and < 7 in. length) or large (> 3 in. diameter and > 12 in. length) size models. For very small sizes (≤ 6 in. large dimension), one may lose the flexibility of nozzle pressure ratio control. The solid propellant simulator concept can be developed for both small and large models to meet design requirements. The liquid monopropellant concept can also be developed in small or large sizes. However, the complexity of its design dictates that the full capabilities (thrust, temperature, on/off operation) of this concept are best realized in

larger scale designs. At the present, in view of the large power required, the laser concept appears to be suited at most to small models with low thrust and mass flow levels.

f. Compatibility With Magnetic Suspension Balance Systems

Here the ease of integrating magnetic material into a design which can serve as the core is important. Also of importance is the thrust rise and fall transient which is estimated to be tens of milliseconds for all concepts. This includes the solid propellant concept with squib ignition. For hot wire ignition, the transients may be of 100 to 400 ms duration. In any case, for a typical sampling rate of 256 Hz (or 4 ms between samples), such as at the University of Southampton MSBS, the transients for all concepts appear to be controllable. This, of course, must be experimentally demonstrated.

g. Compatibility With Wind Tunnel Facilities - General

This criterion deals with the issue of whether the exhaust products from the propulsion simulator are allowed to be entrained in the wind tunnel airstream. In most applications, the mass flow rate from the simulator will be at least two orders of magnitude less than the mass flow rate of air in the test section. Therefore, the exhaust products will be effectively diluted. In open circuit tunnels, the contaminated airstream will leave the tunnel and can be directed outside the building, if necessary. For a closed circuit tunnel, the air contaminated with exhaust products will return, but again the concentration of contaminants will be negligible.

h. Compatibility With Specific Wind Tunnels

This criterion addresses the issue of compatibility of a propulsion simulation concept with current and future MSBS wind tunnels. Here compatibility is evaluated in an overall sense, i.e., it includes the aspects (e), (f), and (g) described above. Four wind tunnels have been selected as representative of small, medium, and large MSBS tunnels using air as working

medium at ambient temperatures, and one large cryogenic wind tunnel. The ambient temperature tunnels currently existing are the University of Southampton 7-in. tunnel (small), and the NASA Langley 13-in. tunnel (medium), and the NASA Langley 8-ft transonic tunnel (large). An 8-ft cryogenic high-speed tunnel has been assumed as a representative future MSBS wind tunnel. Except for the cryogenic tunnel, where the materials in the exhaust products of propulsion simulators may be restricted due to condensation considerations, the compatibility of a concept with various tunnels is based on the model size that can be mounted, and also on whether that size can accommodate a given simulator concept as in (e) above.

i. Safety Risk to Facility and Personnel

This criterion addresses the level of risk to which a propulsion simulator technique exposes the wind tunnel and other equipment as well as facility operators. The liquid and solid propellant simulator concepts are deemed to have somewhat higher level of risk, but this can be mitigated with proper procedures.

j. Cost

Clearly, the simplest compressed CO_2 concept is the cheapest, and one utilizing a high powered laser is the most expensive. The solid and liquid propellant simulators fall inbetween. The solid propellant concept has a large upfront development cost, according to Morton Thiokol (up to \$100 K), making it much more expensive than anticipated cost of the liquid propellant concept (approximately \$50 K).

Table 9 summarizes the comparison of various simulator concepts in terms of the above criteria.

Table 9. Comparative Evaluation of Propulsion Simulator Concepts

Criterion	Compressed Gas	Liquid Mono-propellant	Solid Propellant	Laser-Assisted
a. Ability to meet design requirements	Med	Med-High	Med	Low
b. Complexity of design	Med	Med-High	Med	Low
c. Technology maturity	High	High	High	Low
d. Support equipment needs	Low	Med	Low	High
e. Compatibility with W/T models				
- Small size	Med	Low	High	Low-Med
- Large size	High	High	High	Low
f. Compatibility with MSBS	High	High	High	High
g. Compatibility with W/T facilities (general, see text)	High	High	High	High
h. Compatibility with specific tunnels				
- Univ. of Southampton - 7 in.	High	Low	Med	Low
- NASA Langley - 13 in.	High	High	High	Low
- NASA Langley - 8 ft (ambient temperture)	High	High	High	Low
- Future - 8 ft cryogenic	Med	Low-Med	Low-Med	Med-High
i. Safety risk	Low	Low-Med	Low-Med	Low
j. Cost	Low	Low-Med	High	High

For a Phase II demonstration, the philosophy should be to design, build, and test the simplest, most compatible (with MSBS wind tunnel), and inexpensive propulsion simulator concept first. It is clear from Table 9 that the compressed CO_2 cylinder is such a concept. To verify its compatibility with MSBS control systems, the simulator can be tested either in the University of Southampton 7-in. tunnel or at NASA Langley 13-in. tunnel. For the Southampton wind tunnel, the small model size may require relaxation by some of design requirements on pressure ratio, thrust, mass flow, etc. The NASA Langley tunnel will permit a reasonable size (e.g., 3 in. diammeter x 12 in. long) simulator to be tested.

The CO_2 propulsion simulator delivers only cold jets. The next stage of development should be at least one hot jet concept. Table 9 shows that either the liquid or the solid propellant concept can be developed and tested and the choice will be dictated by practical considerations of cost, difficulty of transporting propellants, etc. The liquid propellant concept has an edge over the solid propellant because the former can be developed to yield multiple (on/off) thrust bursts.

Finally, the laser propulsion simulator concept should be investigated at some level in Phase II. In Table 9, this concept appears the least favorable largely due to the fact that its technical maturity is low at this time. It appears worthwhile to especially test highly ablating materials for the concept shown in Figure 17a. Here, inert and chemically active materials with low heat of vaporization and low specific heat should be investigated. Further, the concept in Figure 17c is promising if a working fluid in the conventional compressed gas concept can be made to absorb laser energy. This will eliminate the present drawback of the latter concept that only cold jets are produced. Laser absorbing gaseous medium such as ammonia should be studied. The objective of diagnostic laser experiments in Phase II should be to find materials which will reduce the currently-projected high power requirements. The potential of the airbreathing propulsion concept should also be investigated further.

5. SUMMARY AND RECOMMENDATIONS

This Phase I SBIR program investigated the feasibility of simulating propulsion-induced aerodynamic effects on scaled aircraft models in wind tunnels employing Magnetic Suspension and Balance Systems (MSBS). The investigation concerned itself with techniques of generating exhaust jets of appropriate characteristics. The influence of aircraft intake was not addressed in this preliminary study. First, general requirements on thrust and mass flow rates were established for typical aircraft engine operating conditions. Various gas generation techniques were then examined to simulate the aircraft propulsive jets. Four basic concepts of propulsion simulators were developed: compressed gas cylinders, liquid propellant gas generators, solid propellant gas generators, and some laser-assisted propulsive thrusters. All concepts were based on considerations of compatibility with wind tunnel models (e.g., compactness), compatibility with MSBS characteristics (e.g., remote-activation, light weight, controllable thrust versus time), and compatibility with wind tunnels facilities (e.g., non-toxic, non-corrosive exhaust). For each propulsion simulator, a conceptual design was developed which identified principal components, mechanism of operation, envelop dimensions, and weight estimates.

Very briefly, the basic ideas behind the four propulsion simulation concepts are as follows. The compressed gas concept uses a pressurized cylinder of liquefied carbon dioxide, which is punctured and the resulting CO_2 vapor at regulated pressure is expanded through a nozzle. This concept is simple, but its limitation is that the jet is cold and temperature effects cannot be simulated. The liquid propellant concept utilizes catalytic decomposition of high purity hydrogen peroxide to produce steam and oxygen at high temperatures (~ 1000°K). Although mechanically more complex, this technique is versatile in producing jets having a range of temperatures and pressure ratios. The solid propellant concept uses a formulation which generates an essentially particle-free jet of very high temperature (~ 2500°K). The main limitation is that the jet cannot be turned off and restarted. Out of a number of laser-assisted propulsion simulation concepts, jet generation by ablating materials

is the most attractive from the viewpoint of mechanical simplicity. Some promising ablator materials were tested to measure their thrust generation and mass flow characteristics under laser irradiation. For all cases, the laser power required was found to be very high (tens of kilowatts) even for the most modest thrust and mass flow levels. Section 4 of this report discusses the foregoing propulsion simulation techniques in more detail.

Finally, a comparative evaluation of various propulsion simulators was made relative to a number of criteria of relevance to a Phase II demonstration, namely, ability to meet design requirements, complexity of design, technology maturity, compatibility with small or large models, compatibility with wind tunnels of different sizes and types, compatibility with magnetic suspension and balance systems, supportability, safety, and cost. Based on this evaluation, the following recommendations are made for demonstrating propulsion simulators in a MSBS wind tunnel in Phase II.

1. Design, build, and test the simplest and the most MSBS-compatible simulator concept first. The compressed liquefied CO_2 concept is the most appropriate. The next stage of development should be a simulator concept which produces high temperature jets. The liquid hydrogen peroxide (H_2O_2) simulation is the best candidate.

2. Verify the compatibility of the above simulators with MSBS control systems in the NASA Langley 13-in. tunnel and/or the University of Southampton 7-in. tunnel. The latter can accept only small (1 in. diam by 6 in. length typically) simulators, which is easier for the compressed CO_2 concept, but not for the liquid H_2O_2 concepts. Therefore, a small scale CO_2 simulator should be tested in the University of Southampton MSBS and a larger scale (3 in. diam x 12 in. length) CO_2 and/or H_2O_2 simulator should be tested in the NASA Langley MSBS. It should be noted that the control systems of both the NASA and Southampton MSBS's will need to be modified to correct for the rapid changes in model position resulting from impulsive thrust forces as the simulator is turned on or off.

3. Bench tests of propulsion simulators should be performed prior to wind tunnel tests. The purpose of bench tests would be to measure thrust versus time characteristics, exhaust jet stagnation temperature and pressure, and to determine jet expansion process photographically. The parameters to be varied should include nozzle area, thrust, mass flow rate, and jet pressure ratio.

4. A modest effort should be spent on the laser-assisted propulsion simulation concepts due to their potential to simulate a variety of propulsive jets and intakes. In particular, impulse and mass flow characteristics of new materials (e.g., highly subliming and chemically active) should be measured in diagnostic experiments. Furthermore, propellant gases which efficiently absorb laser energy should be researched and identified as working fluids in the conventional compressed gas concept. If such working fluids exist, a major drawback of the compressed gas concept, i.e., only cold jets can be generated, will be eliminated. Finally, the potential of continuous wave lasers for the airbreathing propulsion concept should be researched.

6. REFERENCES

1. Lawing, P.L., et al., "Potential Benefits of Magnetic Suspension and Balance Systems," NASA TM 89079, February 1987.

2. Joshi, P.B., et al., "Generic Thrust Reverser Technology for Near-Term Application," Volumes I-IV, AFWAL TR-84-3094, Air Force Wright Aeronautical Laboratories, Wright-Patterson AFB, Ohio, February 1985.

3. Sutton, G.W., Rocket Propulsion Elements, John Wiley, New York, 1957.

4. FMC Corporation, "Hydrogen Peroxide," Technical Bulletin 141 069CPG4875, Philadelphia, PA, 1987.

5. Cleaver, A.V., "Using Hydrogen Peroxide," British Interplanetary Society, London, 1954.

6. Davis, N. and Keefe, J., "Experiment for Use with High-Strength Hydrogen Peroxide," J. American Rocket Society, Vol. 22, No. 63, 1952.

7. Sanz, M.C., "Five-Pound Thrust Liquid Mono-Propellant Rocket," ARS Journal, Vol. 74, September-October, 1948.

8. Scatterfield, C.N. and Sarda, P.K., "Rates of Catalytic Decomposition of Liquid Hydrogen Peroxide on Metal Surfaces," MIT Report No. 58, ONR Contracts NR-092-008 and NONR 1841(11), November 1960.

9. Davis, N. and McCormick, J., "Design of Catalyst Packs for the Decomposition of Hydrogen Peroxide," ARS Propellants, Combustion, and Liquid Rockets Conference, Columbus, Ohio, July 18-19, 1960.

10. Holtzmann, R.T., Chemical Rockets, Marcel Dekker, New York, 1969.

11. Brundige, Winston, Director of Engineering, Morton Thiokol, Inc. Elkton Division, MD, Personal Communication, August 1988.

12. Kantrowitz, A., "Propulsion to Orbit by Ground-Based Lasers," Astronautics and Aeronautics, Vol. 10, No. 5., May 1972, p. 74.

13. Weiss, R.F., Pirri, A.N., and Kemp, N.H., "Laser Propulsion," Astronautics and Aeronautics, March 1979, pp. 50-58.

14. Douglas-Hamilson, Katrowitz, A.R., and Keilly, D.A., "Laser-Assisted Propulsion Research," Radiation Energy Conversion in Space, Progress in Astronautics and Aeronautics, Vol. 61, 1978, pp. 271-278.

15. Rollins, C., et al., "Issues in Laser Propulsion," Physical Sciences Inc., Scientific Report PSI-1036/SR-334, 1988, Andover, MA.

16. Pirri, A.N., et al., "Propulsion by Absorption of Laser Radiation," AIAA J., Vol. 12, No. 9, September 1974.

17. Simons, G.A. and Pirri, A.N., "The Fluid Mechanics of Pulsed Laser Propulsion," AIAA J., Vol. 15, No. 6, June 1977.

18. Rosen, D., et al., "Absorption of CO_2 Laser by Ammonia," Physical Sciences Inc. Technical Report PSI TR-371 under AFOSR Contract F49620-83-C-0039, March 1984.

NASA
National Aeronautics and Space Administration

Report Documentation Page

1. Report No.	2. Government Accession No.	3. Recipient's Catalog No.
NASA CR-182093		

4. Title and Subtitle

Propulsion Simulation for Magnetically Suspended Wind Tunnel Models

5. Report Date

October 1990

6. Performing Organization Code

7. Author(s)

Prakash B. Joshi, Henry P. Beerman, James Chen, Robert H. Krech, Andrew L. Lintz, and David I. Rosen

8. Performing Organization Report No.

PSI-2055/TR-859

10. Work Unit No.

324-01-00

9. Performing Organization Name and Address

Physical Sciences Incorporated
Research Park, Box 3100
Andover, MA 01801

11. Contract or Grant No.

NAS1-18616

12. Sponsoring Agency Name and Address

NASA
Langley Research Center
Hampton, VA 23665-5225

13. Type of Report and Period Covered

Contractor Report
Final 1/88-9/88

14. Sponsoring Agency Code

15. Supplementary Notes

Technical Representative of the Contracting Officer: Pierce L. Lawing, Langley Research Center
SBIR Phase I Final Report

16. Abstract In the Phase I program, Physical Sciences Inc. (PSI) investigated the feasibility of simulating propulsion-induced aerodynamic effects on scaled aircraft models in wind tunnels employing Magnetic Suspension and Balance Systmes (MSBS). The investigation concerned itself with techniques of generating exhaust jets of appropriate characteristics. The influence of aircraft intakes was not addressed in the preliminary study. The objectives of Phase I were to: (1) Define thrust and mass flow requirements of jets, (2) Evaluate techniques for generating propulsive gas within volume limitations imposed by magnetically-suspended models, (3) Conduct simple diagnostic experiments for techniques involving new concepts, (4) Recommend experiments for demonstration of propulsion simulation techniquest in Phase II.

PSI evaluated various techniques of generating exhaust jets of appropriate characteristics on scaled aircraft models in wind tunnels with Magnetic Suspension and Balance Systems (MSBS). Four concepts of remotely-operated propulsion simulators were examined. Three conceptual designs involving innovative adaptation of convential technologies (compressed gas cylinders, liquid, and solid propellants) were developed. The fourth innovative concept, namely, the laser-assisted thruster, which can potentially simulate both inlet and exhaust flows, was found to require very high power levels for small thrust levels. This concept needs further research. Finally, a comparative evaluation of various propulsion simulators was made relative to a number of criteria of relevance to a Phase II demonstration.

17. Key Words (Suggested by Author(s))

Propulsion Simulation, Jet/Free Stream Interactions, Magnetic Suspension Wind Tunnels

18. Distribution Statement

Unclassified - Unlimited

Subject Category 09

19. Security Classif. (of this report)	20. Security Classif. (of this page)	21. No. of pages	22. Price
Unclassified	Unclassified	71	A04